1994). For PCR analysis, nine μl of PCR reaction buffer containing 0.1 μl of recombinant *Taq* DNA polymerase at 5 U/μl (*TaKaRa Taq*™; No. R001A, Takara Shuzo Co., Ltd., Shiga, Japan) was mixed with 1 μl of genomic DNA (approximately 0.5 μg), and the reaction mixture was used for PCR. Forty cycles of PCR were performed with cycle times of 1 min at 94°C, 1 min at 56°C, and 4 min at 72°C. The primers used for amplification of the sequences between the 3′ portion of the 2nd intron of the rabbit β-globin gene and the 5′ region of luc cDNA in the Cre-excised pCTL were βA-S and luc-2RV (Fig. 1B). βA-S (5′-GTG TGA CCG GCG GCT CTA GAG-3′) corresponds to a junctional region between the 1st intron of the chicken β-actin gene and the 2nd intron of the rabbit β-globin gene in pCAGGS (Niwa et al., 1991), and luc-2RV (5′-TCT GCC AAC CGA ACG GAC ATT-3′) corresponds to nucleotides from 1,841 to 1,821 of the firefly luc cDNA in pMAMneo-LUC (GenBank Accession No. U02448). The primers used for amplification of the sequences corresponding to the 5′ portion of luc cDNA in the luc-expression plasmid were luc-S and luc-2RV (Fig. 1B). luc-S (5′-TTA CAT TCT TGA ATG TCG CTC-3′) corresponds to nucleotides from 1,593 to 1,613 of luc cDNA in pMAMneo-LUC (GenBank Accession No. U02448). PCR with luc-S and luc-2RV is expected to yield 249-bp products from luc-expression plasmid. The sequence obtained from PCR of the intact pCTL (without Cre-mediated excision) with the βA-S/luc-2RV primer set is too long to amplify in this assay, but can be amplified after the *loxP*-flanked CAT sequence is removed in pCTL, producing a 471-bp DNA fragment. Products of the reaction were analyzed by electrophoresis in a 2% agarose gel. The gels were stained with ethidium bromide (EtBr), and the amplified DNA bands were visualized by ultraviolet transillumination. As a positive control, 5 ng of pCL DNA was used. As a negative control, 0.5 μg of genomic DNA from untreated mouse-tail was used.

Gene Transfer to Oviductal Epithelium by In Vivo Electroporation (EP)

Intraoviductal injection was performed as described previously (Sato, 2005). One μl of solution containing plasmid DNA and trypan blue (TB; 0.05% final concentration) was slowly injected with a glass micropipette, which had been attached to a mouth-piece, into the ampulla of an oviduct of adult B6C3F1 (CLEA Japan, Inc., Tokyo, Japan) females. These females had been induced to superovulate 2 days previously by administration of eCG (Serotropin; Teikoku Zohki, Tokyo, Japan). The DNA introduced per oviduct was pCE-29 (0.2 μg) + phRL-SV (0.02 μg), pCTL (0.2 μg) + phRL-SV (0.02 μg), pCAG/NCre-5 (0.2 μg) + phRL-SV (0.02 μg), or pCTL (0.2 μg) + pTK/Cre-5 (0.2 μg) + phRL-SV (0.02 μg). The phRL-SV, in which expression of *Renilla reniformis* luc is driven by the SV40 early promoter, was from a kit [Dual-Luciferase Reporter Assay System (No. E1910); Promega Co.] used to normalize for transfection efficiency. After injection, the micropipette was rapidly removed. The oviductal regions were then subjected to in vivo EP. Eight square-wave pulses with a pulse duration of 50 msec and electric field intensity of 50 V were administered from a square-wave pulse generator (T820; BTX Genetronics, Inc., San Diego, CA). One day after in vivo EP, the oviducts were subjected to observation for fluorescence and then weighted. These samples were deep-frozen prior to lysis for measurement of luc activity, as shown below. A total of six oviducts (three females) were electroporated for each transfection group.

Gene Delivery In Vivo Via Tail Vein

Tail vein-mediated gene transfer was performed using the method of Nakamura et al. (2004). Briefly, a mixture of 25 μg of single plasmid DNA was mixed with 50 μl of DMRIE-C (Invitrogen), and the mixture was immediately injected by needle via the tail vein of adult B6C3F1 females. For injection of two circular plasmids, DNA (12.5 μg each) was mixed with 50 μl of DMRIE-C and used. Injections were performed six times (once per day). Four days after the final injection, major organs including brain, liver, heart, kidney, lung, intestine, skeletal muscle, and pancreas were dissected from these treated mice, weighed, and then frozen prior to measurement for luc activity. Four to six females were subjected to in vivo transfection in each transfection group.

Luciferase Assay

Luc assay was performed using a Promega Dual-Luciferase Reporter Assay System kit. The tissues (about 1 g) isolated from mice subjected to tail vein-mediated gene transfer or oviducts 1 day after gene transfer were homogenized in 1 ml of 1× reporter lysis buffer (Promega Co.). After centrifugation at 15,000 rpm for 10 min at 4°C, the supernatant (200 μl) was transferred to a fresh Eppendorf tube. Cells, 1 day after transfection, were collected with a cell scraper and precipitated after brief centrifugation. Cell pellets were then lysed with 1 ml of 1× reporter lysis buffer. Relative light units (RLU) obtained with luc were measured for 5 sec following a 2-sec delay after the addition of the lysate (10 μl) to 50 μl of luc assay substrate (Promega Co.) using a luminometer (TD-20/20; Turner Designs Instruments, Sunnyvale, CA). RLU values were normalized to micrograms of tissue protein added in the luc assay. Tissue protein determinations were performed using Bradford reagent (Bio-Rad Laboratories, Inc., Hercules, CA).

RESULTS

Comparison Between Strong and Weak Promoters in Driving of EGFP Expression In Vitro

The Cre-*loxP* system is a unique system that permits conditional induction of recombination events in a reporter *loxP* site-containing construct. If co-transfection with the reporter construct (pCTL) and the construct carrying tissue-specific promoter-driven Cre gene into

cells is performed, Cre expressed from an introduced vector removes the floxed CAT sequence in pCTL and luc expression commences (as shown schematically in Fig. 1B). Prior to testing the Cre-*loxP*-mediated co-transfection method, which permits enhancement of gene expression from a weak promoter, we evaluated the strength of promoters in the two EGFP-expressing constructs, pCE-29 and pTE (Fig. 1A). pCE-29 has CAG promoter, which is known to be a strong promoter (Niwa et al., 1991; Ishii et al., 1994; Sato et al., 1997), while pTE has HSV-*tk* promoter, known to be a relatively weak promoter (Allen et al., 1988). Transient transfection with single pCE-29 frequently resulted in generation of cells with bright EGFP-derived fluorescence (arrows in Fig. 2a). In contrast, pTE gave rise to poor fluorescence after transfection (arrowheads in Fig. 2c). FACS analysis confirmed the above findings. The percentage of cells transfected with pCE-29 with strong EGFP expression was a mean of 6.35% (Fig. 2d), while in cells transfected with pTE it was below 1.5% (Fig. 2f). We therefore used CAG and HSV-*tk* promoters as strong and weak ones, respectively, as a model for testing our co-transfection approach to enhancement of gene expression using the Cre-*loxP* system. Co-transfection with pCTE and pTC resulted in increase in the number of cells exhibiting high degrees of fluorescence (arrow in Fig. 2b). FACS analysis demonstrated that the mean percentage of cells expressing EGFP strongly after co-transfection with pCTE and pTC was roughly intermediate (4.06%; Fig. 2e) between those of cells transfected with pCE-29 and with pTE, as expected.

Luc Activity in NIH3T3 Cells After Transfection With Several Luc-Expression Plasmids

A comparison of the above two promoters (CAG and HSV-*tk*) together with another podocyte-specific nephrin promoter in NIH3T3 cells was also performed in a transient luc expression assay. As shown in Figure 3, activity was clearly obtained with the CAG promoter-driven luc expression construct (pCL), which yielded the highest expression of luc. Moderate activity was seen when cells were transfected with luc-expression construct (pTL) carrying HSV-*tk* promoter. The strength of the CAG promoter was approximately 43-fold that of the HSV-*tk* promoter. Co-transfection of reporter construct (pCTL) and Cre-expressing plasmid pTC resulted in

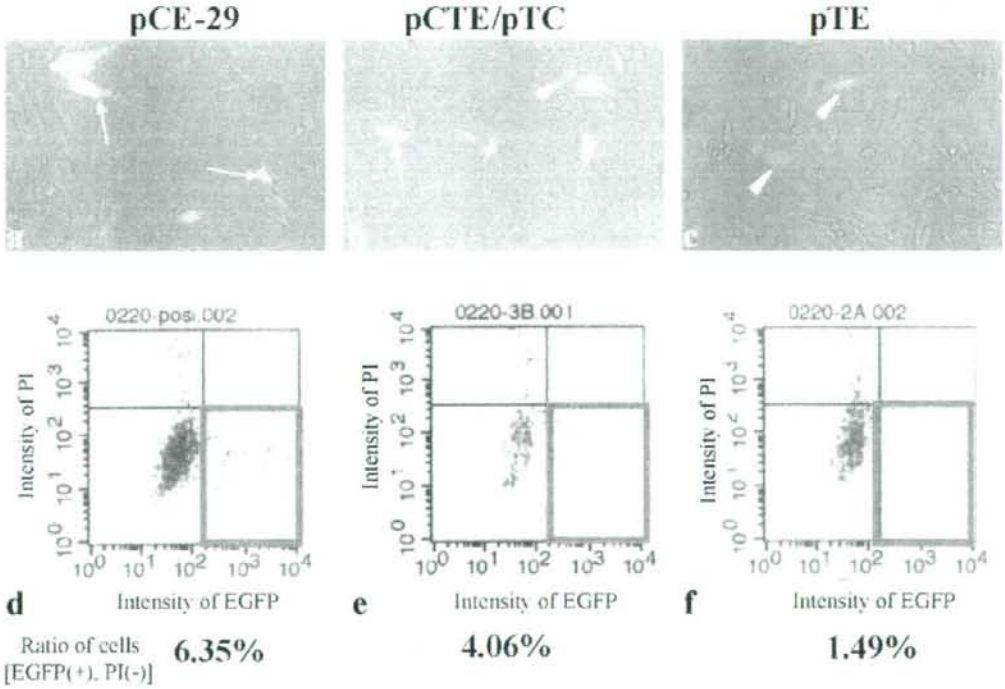

Fig. 2. Comparison between CAG and HSV-*tk* promoters. **a–c**: Microphotographs taken under ultraviolet (UV) light and room light. NIH3T3 cells were transfected with pCE-29/Lipofectamine 2000 complex (a), pCTE/pTC/Lipofectamine 2000 complex (b), and pTE/Lipofectamine 2000 complex (c), and 1 day after transfection cells were inspected. Arrows indicate cells exhibiting strong fluorescence, and arrowheads cells exhibiting weak fluorescence. **d–f**: FACS analysis of cells transfected with vectors shown in (a–c) 1 day after transfection. The percentage of cells exhibiting strong fluorescence (corresponding to the area surrounded by the blue line) was calculated as the number of cells exhibiting strong fluorescence per number of cells exhibiting strong fluorescence + number of cells exhibiting weak fluorescence.

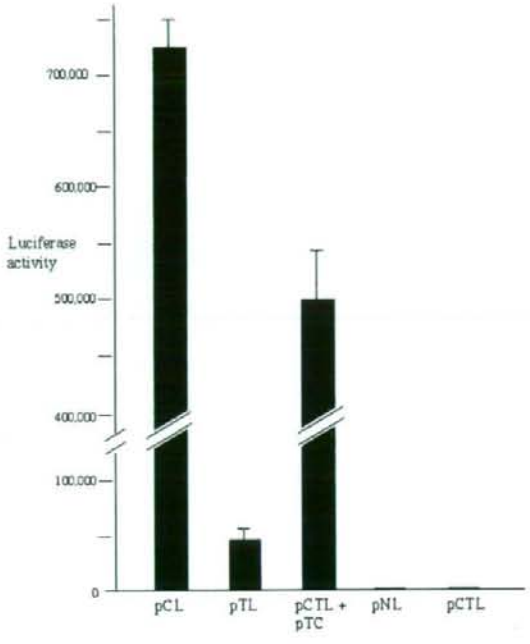

Fig. 3. Luc activity in NIH3T3 cells after transient transfection of luc reporter constructs. The cells (2×10^6) were transfected with luc expression plasmid(s) + phRL-SV encapsulated by Lipofectamine 2000. One day after transfection, cells were lysed for measurement of luc activity. Values were standardized individually for each transfection group using a SV40 promoter-containing construct (phRL-SV) and shown as RLU. The values shown are means for three different experiments. Error bars indicate standard deviations. pCL, cells transfected with pCL + phRL-SV; pTL, cells transfected with pTL + phRL-SV; pCTL + pTC, cells transfected with pCTL + pTC + phRL-SV; pNL, cells transfected with pNL + phRL-SV; pCTL, cells transfected with pCTL + phRL-SV.

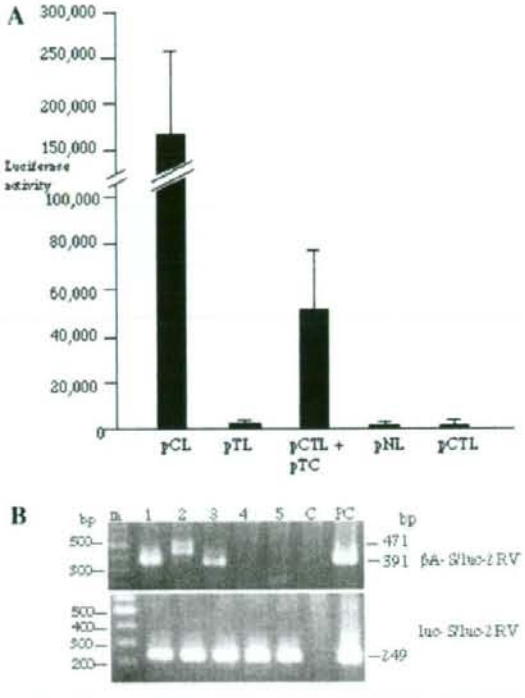

Fig. 4. A: Cre-mediated excision in vivo. Oviducts were transfected by in vivo electroporation with luc expression plasmid(s) + phRL-SV, and 1 day later luc activity in the oviducts was measured. pCL, cells transfected with pCL + phRL-SV; pTL, cells transfected with pTL + phRL-SV; pCTL + pTC, cells transfected with pCTL + pTC + phRL-SV; pNL, cells transfected with pNL + phRL-SV; pCTL, cells transfected with pCTL + phRL-SV. Four oviducts were tested per transfection group, and results are expressed as mean ± SEM. **B**: PCR analysis of genomic DNA derived from gene transfer to mouse oviducts using primers (βA-S/luc-2RV and luc-S/luc-2RV). Note the presence of a 471-bp band, evidence for Cre-mediated recombination in pCTL, in the samples co-transfected with pCTL and pTC (lane 2). PCR with luc-S/luc-2RV primers generated a 249-bp band, indicating the presence of exogenous luc-expression plasmid in the transfected samples. Lane 1, oviduct transfected with pCL + phRL-SV; lane 2, oviduct transfected with pCTL + pTC + phRL-SV; lane 3, oviduct transfected with pTL + phRL-SV; lane 4, oviduct transfected with pNL + phRL-SV; lane 5, oviduct transfected with pCTL + phRL-SV; lane C, intact oviduct (without DNA transfection); lane PC, pCL DNA (5 ng) as a positive control. "m" indicates 100-bp ladder markers.

increased luc activity (approximately 10-fold that with transfection with pTL). Transfection with pNL (carrying mouse nephrin promoter + luc cDNA) resulted in very low levels of luc activity similar to that with the reporter alone (pCTL). These findings indicate that the Cre-*loxP*-mediated co-transfection system works well in vitro for enhancement of gene expression from a weak promoter.

Luc Activity in Oviducts After Gene Delivery and Molecular Analysis of Cre-Mediated Recombination

We next examined whether Cre-*loxP* system-mediated enhancement of gene expression using pCTL as a reporter plasmid can also be used in vivo. For this purpose, gene delivery into murine oviductal epithelium was performed by DNA injection into the lumen of oviducts and subsequent EP (Sato, 2005). One day after gene transfer, oviductal samples were dissected, weighed, and homogenized to examine luc activity. The results are shown in Figure 4A. As expected, instillation of single pCL plasmid yielded a high degree of luc activity. When pTL was singly introduced, only slight luc activity was observed. Co-expression of pCTL and pTC yielded luc activity about 16-fold higher than expression of pTL alone. Only residual levels of luc activity were observed when pNL or pCTL plasmid DNA was singly introduced. These findings indicate that the Cre-*loxP* system using pCTL as a reporter construct works well even in vivo.

Cre-mediated recombination in the introduced pCTL was also confirmed by molecular biological analysis. Genomic DNA from the oviductal samples isolated 1 day

after gene delivery was subjected to PCR using βA-S and luc-2RV or luc-S and luc-2RV as primers (Fig. 1B). PCR using the former primer set should yield 471-bp products if Cre-mediated recombination occurs in the pCTL plasmid. The product derived from intact pCTL could not be visualized in a gel electrophoretic assay because its size (>2 kb) is too large for successful amplification in our PCR system. PCR with the latter primer set should yield 249-bp products corresponding to the 5′ region of luc cDNA if the oviductal samples possess the plasmid DNA injected. As expected, PCR using βA-S and luc-2RV primers revealed that only the samples co-introduced with pCTL and pTC exhibited the 471-bp band (lane 2 in the upper column of Fig. 4B). Furthermore, all the tested samples that had been injected with luc expression vectors had the exogenous DNA (lower column in Fig. 4B).

Luc Activity in Major Organs After Repeated Intravenous Injection of Liposome-Encapsulated Plasmids

We next examined whether the Cre-*loxP* system-based co-transfection method could confer enhanced expression of a target gene in vivo in a tissue-specific fashion. In this case, we aimed to force expression of luc specifically in renal podocytes using pCTL and pNC (carrying the NCre gene linked to the upstream nephrin promoter) (Fig. 1A). Repeated intravenous injections of plasmid DNA encapsulated by liposomes (six times in total; one injection per day) were performed, since this yielded systemic expression of the exogenous gene in various organs such as kidney, intestine, lung, and heart (Nakamura et al., 2004). Adult females were injected with pCL alone, pCTL + pTC, pTL alone, pNL alone, or pCTL + pNC, each of which had been included with phRL-SV and complexed with the liposomal reagent DMRIE-C. Four days after the final injection, organs were dissected and subjected to measurement of luc. The results are shown in Figure 5. Introduction of pCL alone yielded high degrees of luc activity in some organs including lung, intestine, kidney, and heart. In contrast, transfection with pTL alone resulted in relatively weak activity of luc in the lung, intestine, liver, kidney, heart, and spleen. As expected, transfection with pCTL + pTC resulted in increase of luc activity, from 1.8-fold to 4.1-fold that with pTL alone in all organs tested. Interestingly, when mice were transfected with pNL alone, kidney alone exhibited slight expression of luc. Co-transfection with pCTL and pNC resulted in increase in luc activity to 2.4-fold that with pNL alone, and as expected, luc activity was restricted to the kidney.

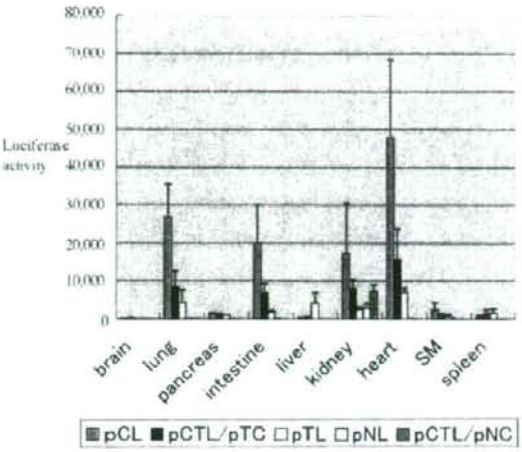

Fig. 5. Effect of co-transfection by repeated intravenous injection of Cre-expression vector on pCTL reporter gene. Twenty-five micrograms of pCTL and 25 μg of Cre expression plasmid (pTC or pNC) or the control plasmid alone (pCL, pTL, or pNL; 25 μg) were co-formulated with 2.5 μg of phRL-SV and 50 μl of DMRIE-C in a total volume of 200 μl and injected intravenously. Six daily injections were performed, and 4 days after the final injection each organ dissected was weighed and homogenized for measurement of luc activity. Each bar is the mean ± SEM (n = 3). SM, skeletal muscle.

DISCUSSION

Strong, long-term expression of delivered foreign or therapeutic genes in specific cell types is an essential requirement for examination of gene function and for experimental gene therapy. Efforts have been made to manipulate vectors to restrict gene expression to specific cell types. This can be achieved in part by employing tissue-specific promoters to drive transcription of a target cDNA. However, as mentioned above, one disadvantage of tissue-specific promoters is the relatively low levels of gene expression obtained compared with viral promoters. In this study, we employed a co-expression approach to restrict enhanced gene expression to specific cell types with a Cre-*loxP* system. The feasibility of this approach was demonstrated by enhancement of transcriptional activity (ca. 10 to 16-fold) in vitro and in vivo, compared to the activity in cells transfected with vectors carrying a weak but ubiquitous HSV-*tk* promoter or podocyte-specific nephrin promoter.

Kaczmarczyk and Green (2001) created a single vector that included all necessary components required for Cre-mediated enhancement of tissue-specific gene expression. In this case, the possibility exists that spontaneous Cre-mediated excision could occur within a single construct, if the promoter used to drive the downstream Cre gene occasionally functions during cloning in *E. coli*. To prohibit unwanted Cre-mediated recombination, they inserted a mutated sequence in the 5′ region of the Cre gene with which the translational start site was optimized for eukaryotic translation using a Kozak consensus sequence, as well as an artificial intron within the Cre coding sequence. These two treatments actually prevented translation of Cre protein in bacteria. They also added chicken β-globin insulators between the two constructs, a construct carrying tissue-specific promoter to drive the expression of Cre, and another unit carrying a

strong promoter + *loxP*-floxed sequence (stop) + a target gene. The addition of insulators reduced potential enhancer effects from a strong transcriptional unit on the relatively weak but tissue-specific expression of Cre.

The co-transfection approach does not require modification of the Cre gene, incorporation of insulators, or connection of different transcriptional units as a single construct. However, the co-transfection protocol has its own potential disadvantage, that not all transduced cells receive an optimal molar ratio of both transcriptional units, with the effector carrying tissue-specific promoter-driven Cre gene and the reporter (tester) carrying strong promoter + *loxP*-floxed sequence + a target gene. This would result in sub-optimal activity and/or specificity. This is probably true in some cases that transfection efficiency is very low. For example, in this study only 10-fold enhancement of gene expression was achieved (see Fig. 3), under the condition where less than 10% of NIH3T3 cells appeared to be in vitro transfected with a lipofection method (see Fig. 2a–c). In contrast, we observed up to 16-fold enhancement of gene expression with in vivo co-transfection toward murine oviductal epithelium (see Fig. 4A). In this case, transfection efficiency might have been higher than that observed in the in vitro-cultured cells. In fact, we previously observed that maximal approximately 40% of oviductal epithelial cells could be successfully transfected by in vivo EP system (Sato, 2005). Co-transfection via the tail vein resulted in from 1.8-fold to 4.1-fold enhancement of expression of a target gene, which may also reflect a low degree of gene transfer efficiency in this system (see Fig. 5).

Another advantage to use of the co-transfection system is that the target gene can be expressed in any tissue if the *loxP* site-containing tester vector (in this case, for example, pCTL) is combined with pre-existing Cre gene-expression vectors (as effectors) carrying tissue-specific promoter. Figure 6 schematically shows examples of this co-transfection system. The tester transgene can be introduced into the mouse genome as a transgenic instead of using co-transfection with effectors. Once transgenics carrying such tester transgene are produced, a target protein can be expressed from the integrated tester transgene in any tissues desired by exogenously adding effector constructs through intravenous injection of DNA or by other transfection methods.

In this study, we succeeded in inducing enhancement (ca. 2.4-fold) of gene expression in a specific cell-type (i.e., podocytes) using the podocyte-specific nephrin promoter by co-injection of liposome-encapsulated pCTL and pNC into mouse-tail vein (see Fig. 5). The histological distribution of luc in podocytes has not yet been determined using anti-luc antibody. However, in a preliminary experiment, we observed podocyte-restricted expression of EGFP, when cryostat sections derived from mice repeatedly receiving liposome-encapsulated pNE (carrying 5-kb nephrin promoter and EGFP cDNA) were examined by a confocal laser scanning microscope (data not shown). We are now testing whether in vivo co-transfection of pCTE and pNC (Fig. 1A) results in visualization of enhanced expression of EGFP in podocytes at the histological level.

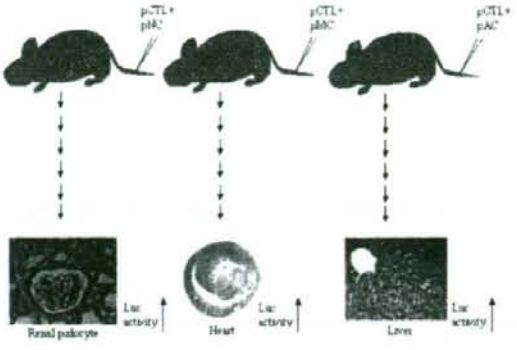

Fig. 6. Advantages of in vivo co-transfection method for enhancement of gene expression in any tissue in which gene transfer is to be performed. Combination of a reporter construct pCTL with a pre-existing Cre-expression plasmid enables targeted and enhanced expression of luc. For example, co-introduction of pCTL and pNC via the tail vein (this study) will result in podocyte-specific luc expression. Co-introduction of pCTL and pMC (carrying myosin heavy chain promoter-driven Cre; Agah et al., 1997) will induce luc expression specifically in heart. Co-introduction of pCTL and pAC (carrying albumin promoter-driven Cre; Herweijer et al., 2001) will induce luc expression specifically in liver.

As mentioned above, there are several methods for enhancement of gene expression with cell-type specificity, including the Cre-*loxP*-based system (Kaczmarczyk and Green, 2001; this study), and insertion of responsive elements (i.e., SRF elements and WPRE) near the tissue-specific promoter (Li et al., 1999; Glover et al., 2002, 2003; Hermening et al., 2004). The latter method is of special interest since it can be simply performed by insertion of such elements near the CAG promoter in our pCTL. Another approach that can improve the strength of a tissue-specific promoter is the use of viral enhancers. Inclusion of an enhancer at the 5′ of a promoter improved the transcriptional activity of a promoter without affecting cell specificity (Liu et al., 2006). Chemical methods using polyethylene glycol (PEG) for enhancement of expression of a foreign gene exogenously administered are also of interest. For example, Ishida et al. (2006) reported the usefulness of PEG for this purpose. It has also been demonstrated that Pluronic block copolymers can increase regional expression of naked plasmid DNA after its injection in skeletal and cardiac muscle (Lemieux et al., 2000; Pitard et al., 2002).

In conclusion, we have demonstrated that Cre-*loxP*-based co-transfection augments gene expression from a weak promoter in vitro and in vivo in different gene delivery systems. The strategy we have developed will have great potential for a wide variety of studies in molecular and cellular biology as well as for future clinical applications.

ACKNOWLEDGMENTS

The authors would like to thank Dr. Kimi Araki (Kumamoto University) for allowing us to use pCAG-CAT-Z plasmid. This study was supported by Grants-in-Aid for Scientific Research (S) (Grant No. 17100007) from the Ministry of Education, Science, Sports, Culture, and Technology of Japan, and also by Grants-in-Aid from the Research on Health Sciences focusing on Drug Innovation (Japan).

REFERENCES

Agah R, Frenkel PA, French BA, Michael LH, Overbeek PA, Schneider MD. 1997. Gene recombination in postmitotic cells. Targeted expression of Cre recombinase provokes cardiac-restricted, site-specific rearrangement in adult ventricular muscle in vivo. J Clin Invest 100:169–179.

Allen ND, Cran DG, Barton SC, Hettle S, Reik W, Surani MA. 1988. Transgenes as probes for active chromosomal domains in mouse development. Nature 333:852–855.

Araki K, Araki M, Miyazaki J, Vassalli P. 1995. Site-specific recombination of a transgene in fertilized eggs by transient expression of Cre recombinase. Proc Natl Acad Sci USA 92:160–164.

Brinster RL, Allen JM, Behringer RR, Gelinas RE, Palmiter RD. 1988. Introns increase transcriptional efficiency in transgenic mice. Proc Natl Acad Sci USA 85:836–840.

Choi T, Huang M, Gorman C, Jaenisch R. 1991. A generic intron increases gene expression in transgenic mice. Mol Cell Biol 11:3070–3074.

Dzojic H, Cheng WS, Essand M. 2007. Two-step amplification of the human PPT sequence provides specific gene expression in an immunocompetent murine prostate cancer model. Cancer Gene Ther 14:233–240.

Emiliusen L, Gough M, Bateman A, Ahmed A, Voellmy R, Chester J, Diaz RM, Harrington K, Vile R. 2001. A transcriptional feedback loop for tissue-specific expression of highly cytotoxic genes which incorporates an immunostimulatory component. Gene Ther 8:987–998.

Glover CP, Bienemann AS, Heywood DJ, Cosgrave AS, Uney JB. 2002. Adenoviral-mediated, high-level, cell-specific transgene expression: A SYN1-WPRE cassette mediates increased transgene expression with no loss of neuron specificity. Mol Ther 5:509–516.

Glover CP, Bienemann AS, Hopton M, Harding TC, Kew JN, Uney JB. 2003. Long-term transgene expression can be mediated in the brain by adenoviral vectors when powerful neuron-specific promoters are used. J Gene Med 5:554–559.

Hermening S, Kugler S, Bahr M, Isenmann S. 2004. Increased protein expression from adenoviral shuttle plasmids and vectors by insertion of a small chimeric intron sequence. J Virol Methods 122:73–77.

Herweijer H, Zhang G, Subbotin VM, Budker V, Williams P, Wolff JA. 2001. Time course of gene expression after plasmid DNA gene transfer to the liver. J Gene Med 3:280–291.

Ishida T, Li W, Liu Z, Kiwada H. 2006. Stimulatory effect of polyethylene glycol (PEG) on gene expression in mouse liver following hydrodynamics-based transfection. J Gene Med 8:324–334.

Ishii M, Tashiro F, Hagiwara S, Toyonaga T, Hashimoto C, Takei I, Yamamura K, Miyazaki J. 1994. Embryonic expression of MHC class I heavy and light chains in transgenic mice. Endocr J 41:S9–S16.

Iyer M, Wu L, Carey M, Wang Y, Smallwood A, Gambhir SS. 2001. Two-step transcriptional amplification as a method for imaging reporter gene expression using weak promoters. Proc Natl Acad Sci USA 98:14595–14600.

Iyer M, Salazar FB, Lewis X, Zhang L, Carey M, Wu L, Gambhir SS. 2004. Noninvasive imaging of enhanced prostate-specific gene expression using a two-step transcriptional amplification-based lentivirus vector. Mol Ther 10:545–552.

Iyer M, Salazar FB, Lewis X, Zhang L, Wu L, Carey M, Gambhir SS. 2005. Non-invasive imaging of a transgenic mouse model using a prostate-specific two-step transcriptional amplification strategy. Transgenic Res 14:47–55.

Kaczmarczyk SJ, Green JE. 2001. A single vector containing modified cre recombinase and LOX recombination sequences for inducible tissue-specific amplification of gene expression. Nucleic Acids Res 29:e56.

Koch PE, Guo ZS, Kagawa S, Gu J, Roth JA, Fang B. 2001. Augmenting transgene expression from carcinoembryonic antigen (CEA) promoter via a GAL4 gene regulatory system. Mol Ther 3:278–283.

Lee M, Oh S, Ahn CH, Kim SW, Rhee BD, Ko KS. 2006. Mitochondrial Research Group. An efficient GLP-1 expression system using two-step transcription amplification. J Control Release 115:316–321.

Lemieux P, Guerin N, Paradis G, Proulx R, Chistyakova L, Kabanov A, Alakhov V. 2000. A combination of poloxamers increases gene expression of plasmid DNA in skeletal muscle. Gene Ther 7:986–991.

Li S, MacLaughlin FC, Fewell JG, Li Y, Mehta V, French MF, Nordstrom JL, Coleman M, Belagali NS, Schwartz RJ, Smith LC. 1999. Increased level and duration of expression in muscle by co-expression of a transactivator using plasmid systems. Gene Ther 6:2005–2011.

Liu BH, Wang X, Ma YX, Wang S. 2004. CMV enhancer/human PDGF-beta promoter for neuron-specific transgene expression. Gene Ther 11:52–60.

Liu BH, Yang Y, Paton JF, Li F, Boulaire J, Kasparov S, Wang S. 2006. GAL4-NF-kappaB fusion protein augments transgene expression from neuronal promoters in the rat brain. Mol Ther 14:872–882.

Moeller MJ, Kovari IA, Holzman LB. 2000. Evaluation of a new tool for exploring podocyte biology: Mouse Nphs1 5′ flanking region drives LacZ expression in podocytes. J Am Soc Nephrol 11:2306–2314.

Nakamura S, Terashima M, Kikuchi N, Kimura M, Maehara T, Saito A, Sato M. 2004. A new mouse model for renal lesions produced by intravenous injection of diphtheria toxin A-chain expression plasmid. BMC Nephrol 5:4.

Nettelbeck DM, Jerome V, Müller R. 1998. A strategy for enhancing the transcriptional activity of weak cell type-specific promoters. Gene Ther 5:1656–1664.

Niwa H, Yamamura K, Miyazaki J. 1991. Efficient selection for high-expression transfectants with a novel eukaryotic vector. Gene 108:193–200.

Pitard B, Pollard H, Agbulut O, Lambert O, Vilquin JT, Cherel Y, Abadie J, Samuel JL, Rigaud JL, Menoret S, Anegon I, Escande D. 2002. A nonionic amphiphile agent promotes gene delivery in vivo to skeletal and cardiac muscles. Hum Gene Ther 13:1767–1775.

Ray S, Paulmurugan R, Hildebrandt I, Iyer M, Wu L, Carey M, Gambhir SS. 2004. Novel bidirectional vector strategy for amplification of therapeutic and reporter gene expression. Hum Gene Ther 15:681–690.

Sato M. 2005. Intraoviductal introduction of plasmid DNA and subsequent electroporation for efficient in vivo gene transfer to murine oviductal epithelium. Mol Reprod Dev 71:321–330.

Sato M, Tada N, Iwase R, Amann E. 1993. Gene introduction into mouse blastocysts via "pricking". Mol Reprod Dev 34:349–356.

Sato M, Iwase R, Kasai K, Tada N. 1994. Direct injection of foreign DNA into mouse testis as a possible alternative of sperm-mediated gene transfer. Animal Biotechnol 5:19–31.

Sato M, Kawarabayashi T, Shoji M, Kobayashi T, Hirai S, Tada N. 1997. Cytomegalovirus enhancer/chicken β-actin promoter confers constitutive and ubiquitous transgene expression in vivo. Transgenics 2:153–159.

Sato M, Watanabe T, Kimura M. 1999. Embryo transfer via oviductal wall: An alternative method for efficient production of transgenic mice. Transgenics 2:383–389.

Sato M, Ishikawa A, Kimura M. 2002. Direct injection of foreign DNA into mouse testis as a possible in vivo gene transfer system via epididymal spermatozoa. Mol Reprod Dev 61:49–56.

Sato M, Johnson M, Zhang L, Zhang B, Le K, Gambhir SS, Carey M, Wu L. 2003. Optimization of adenoviral vectors to direct highly amplified prostate-specific expression for imaging and gene therapy. Mol Ther 8:726–737.

Artificial Organs

Artificial Organs
33(1):74–85, Wiley Periodicals, Inc.

Thoughts and Progress

Photocrosslinkable Chitosan Hydrogel Can Prevent Bone Formation in Both Rat Skull and Fibula Bone Defects

*Yoshifumi Tsuda, †Masayuki Ishihara, *Masatoshi Amako, *Hiroshi Arino, †Hidemi Hattori, †Yasuhiro Kanatani, ‡Hirofumi Yura, and *Koichi Nemoto

*Department of Orthopaedic Surgery, National Defense Medical College; †Division of Biomedical Engineering, Research Institute, National Defense Medical College, Tokorozawa, Saitama; and ‡NeTech Inc. KSP, Sakado, Takatsu, Kawasaki, Kanagawa, Japan

Abstract: UV light irradiation to a photocrosslinkable chitosan (Az-CH-LA) resulted in an insoluble and flexible hydrogel within 30 s. The purpose of this study was to evaluate the ability of the photocrosslinkable chitosan to inhibit bone formation in the bone defects. A 5-mm-diameter defect was made in the rat calvarium, and then photocrosslinkable chitosan was implanted and irradiated with UV for 30 s. Furthermore, a 2-mm defect was made in the fibula of a rat hind leg, and then photocrosslinkable chitosan was implanted and irradiated with UV. Bone formations in the rat skull and fibula defects with photocrosslinkable chitosan hydrogel were significantly prevented for 8 weeks. Thus, the chitosan hydrogel has an inhibitory effect on bone formation. **Key Words:** Bone formation—Hydrogel—Photocrosslinkable chitosan—Synostosis—Tissue engineering.

Recent progress in regenerative medicine raises the hope that bone defects can be treated with a combination of biomaterials and growth factors (1). However, orthopedic surgeons sometimes treat cases in which bone formation needs to be inhibited rather than stimulated (2). For example, congenital radioulnar synostosis results in loss of forearm rotation and functional disability of the upper limb due to bone union of the proximal radioulnar joint (2). Resection of the synostosis and interposition of fat, muscle, or silicon sheet have been tried to restore rotation; however, postoperative re-union was inevitable (2). Heterotopic ossification often occurs after fractures, burns, and spinal cord injuries, and this is one of the major orthopedic problems to be solved because this leads to considerable functional disability (3). Surgical excision of the ectopic bone is more complicated when the ectopic bones are large and complicated around the joints. If a material could be found that can inhibit bone formation, then treatment for these problems must be easier. The material to prevent bone formation needs to be a good filler of bone defect, slowly biodegradable, and biocompatible. However, at present, there is no satisfactory material for preventing bone formation.

Chitin is a linear homopolymer of 1, 4β-linked N-acetyl-D-glucosamine, and chitosan is a partially deacetylated chitin (4). Due to their biocompatibility, chitin and chitosan have been proposed for use as biomaterials in a range of biomedical and industrial applications (5). We have reported previously the preparation and characterization of a novel photocrosslinkable chitosan (4,5). The material is a viscous solution and is easily crosslinked upon UV light irradiation which results in the formation of an insoluble hydrogel within 30 s (4,5). In this article, we demonstrated that chitosan hydrogel had a significant inhibitory effect on bone formation.

MATERIALS AND METHODS

Preparation of photocrosslinkable chitosan molecules (Az-CH-LA)

Az-CH-LA was prepared as previously described (4) using chitosan with a molecular weight of $0.8^{-1} \times 10^6$ Da and a deacetylation ratio of 0.8 (DAC-80). Azide (p-azidebenzoic acid) and lactose (lactobionic acid) moieties were introduced through a condensation reaction with amino groups. A viscous Az-CH-LA aqueous solution has been converted into an insoluble hydrogel within 30 s upon UV irradiation at a lamp distance of 2 cm through crosslinking of the azide and amino groups of the Az-CH-LA molecules (5).

Experimental procedure and evaluation of the inhibition of bone formation

Male, 6-week-old Sprague-Dawley rats were obtained from Charles River Laboratories (Tokyo, Japan). The National Medical Defense College

doi:10.1111/j.1525-1594.2008.00676.x

Received November 2007; revised December 2007.

Address correspondence and reprint requests to Dr. Masayuki Ishihara, Division of Biomedical Engineering, Research Institute, National Defense Medical College, 3-2 Namiki, Tokorozawa, Saitama 359-8513, Japan. E-mail: ishihara@ndmc.ac.jp

Animal Care and Use Committee have approved all experimental procedures prior to their use. Animals were anesthetized with an intraperitoneal injection of a 5% pentobarbiturate solution (1 mg/mL).

The animal's head was cut to expose the skull bone, and periosteum of the calvarium was abraded. Without injuring the underlying dura mater and mid-sagittal blood sinus, we carefully made full-thickness skull defects, 5 mm in diameter, by trephine (RS-9200, Roboz Surgical Instruments Co., Inc., Gaithersburg, MD, USA). The critical size defect of the rat skull bone was considered as 8 mm in diameter (6,7). The chitosan hydrogels were placed in the defects and fixed by UV irradiation. Untreated animals were processed in the same way, but nothing was implanted after the defects were created. After the treatment, the abraded periosteum was sutured with 5-0 nylon monofilaments and the skin was sutured with 3-0 nylon monofilaments. No antibiotics were used; no bacterial infection occurred after surgery. To reach the fibula, we made a skin incision in the posterior and distal part of the hind legs. The fascia of the flexor muscles was incised and fibula was exposed without injuring the flexor muscles. The distal part of the rat fibula was fused with the tibia. The critical size defect of the rat fibula bone was considered as 4 mm (8). A 2-mm segment of the distal part of the fibula was excised, and the chitosan hydrogels were placed in the osteotomy site and fixed by UV irradiation. The contralateral fibula was processed in the same manner but nothing was implanted in the osteotomy site. After the treatment, the fascia was sutured with 5-0 nylon monofilaments and the skin was sutured with 3-0 nylon monofilaments. No antibiotics were used; no bacterial infection occurred after surgery.

Four and 8 weeks after surgery, the animals were sacrificed by an intraperitoneal injection of an overdose of a 5% pentobarbiturate solution. The skull and fibula were removed and fixed in 10 wt% formaldehyde solution for 2 days. The radiographic assessments of the skull and fibula defect were carried out using soft X-ray (Softex CSM-2, 30KV, 10 mA, 15 s, Softex Co., Inc., Kanagawa, Japan). The soft X-ray examination was performed at 4 and 8 weeks after surgery. The areas of the skull bone defect and the length of the fibula bone defect were calculated by using NIH Image (version 1.16, Scion Corporation, Frederick, MD, USA). All data were analyzed by Student's *t*-test; P values less than 0.05 were considered to be statistically significant.

RESULTS

Figure 1A shows soft X-ray films of rat skull bone defects that were obtained 4 and 8 weeks after surgery. The remaining chitosan hydrogels were observed in the skull bone defects treated with photocrosslinkable chitosan hydrogels at 4 and 8 weeks (data not shown). However, in the untreated group, newly formed bone was found 4 weeks after surgery and gradually increased up to 8 weeks, although it did not fill the bone defect completely. Figure 1B shows the areas of the skull bone defects evaluated using radiographic analysis. The mean areas were 16.5 mm^2 in the experimental group and 14.0 mm^2 in the control group 4 weeks after surgery, and 14.8 mm^2 in the experimental group and 10.1 mm^2 in the control group 8 weeks after surgery ($P < 0.05$).

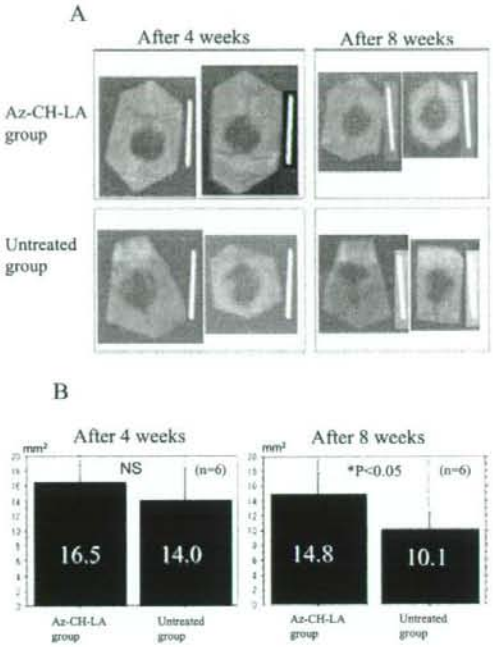

FIG. 1. Soft X-ray films of rat skull bone defects that were obtained 4 and 8 weeks after surgery (A). The photographs (A) include six representative chitosan hydrogel-treated- and control bone defects. The chitosan hydrogels that were implanted were still present in skull bone defects 4 and 8 weeks after surgery, while in control, a newly formed bone was found 4 weeks after surgery and gradually increased up to 8 weeks. The areas of the skull bone defects were evaluated using radiographic analysis (B). The data are presented as the mean ± SD. *$P < 0.05$, versus control, unpaired Student's *t*-test ($n = 6$).

Figure 2A shows soft X-ray films of the rat fibula bone defects that were obtained 4 and 8 weeks after surgery. As seen with the skull bone defects, the chitosan hydrogels were observed in the fibula defects treated with photocrosslinkable chitosan hydrogels

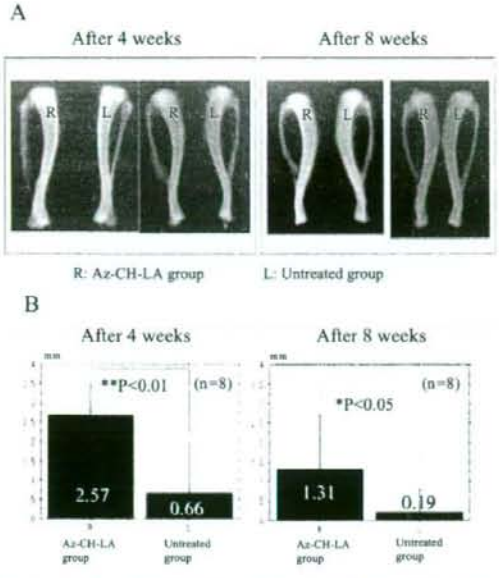

FIG. 2. Soft X-ray films of rat fibula bone defects which were obtained 4 and 8 weeks after surgery (A). The photographs (A) include six representative chitosan hydrogel-treated- and control bone defects. The chitosan hydrogels that were implanted were still present in fibula bone defects 4 and 8 weeks after surgery, while the untreated control fibula defects were completely bridged by a newly formed bone 8 weeks after surgery. The length of the fibula bone defects was evaluated by using radiographic analysis (B). The data are presented as the mean ± SD. $^{*}P < 0.05$, $^{**}P < 0.01$, versus control, unpaired Student's *t*-test ($n = 8$).

at 4 and 8 weeks (data not shown). However, the untreated fibula defects were completely bridged by a newly formed bone at 8 weeks. Figure 2B shows the length of the fibula bone defects evaluated using radiographic analysis. The mean lengths were 2.57 mm in the experimental group and 0.66 mm in the control group at 4 weeks after surgery, and 1.31 mm in the experimental group and 0.19 mm in the control group at 8 weeks after surgery. The differences between the groups were statistically significant at both 4 and 8 weeks after surgery ($P < 0.05$).

DISCUSSION

We have reported previously that a photocrosslinkable chitosan hydrogel was useful as a biological adhesive and defect filler (5,8). When the photocrosslinkable chitosan hydrogel was implanted into rat skull and fibula defects, bone regenerations in the defects were strongly inhibited for at least 8 weeks. This observation suggested that photocrosslinkable chitosan hydrogel was a useful biomaterial that could prevent the formation of the ectopic bone formation that might occur as an unpredictable result after a bone and joint surgery.

Chitin and chitosan are known as a biodegradable and nontoxic natural polymer that enhances wound healing (8,9). Furthermore, chitosan membrane (10), nanofiber (11), and sponge (12) have been produced as tissue-engineering scaffolds for bone formation. However, chitin (chitosan) changes its physical and biological properties according to its deacetylation level (13). When mouse osteoblast cells were cultured on sheets made of nondeacetylated chitin, and 35, 50, and 70% deacetylated chitin (DAC-0, DAC-35, DAC-50, and DAC-70, respectively), DAC-35 had the highest effect of growth and differentiation of the cells, and DAC-50 and DAC-0 had intermediate effects, while DAC-70 suppressed the growth and differentiation of the cells (13). In the present study, DAC-80 chitin (chitosan) was used to prepare photocrosslinkable chitosan hydrogel. Similarly to the DAC-70 chitosan, the DAC-80 chitosan was used to prepare photocrosslinkable chitosan hydrogel to suppress differentiation of osteoblast cells (data not shown).

Although it has been reported that neutrophils could degrade chitosan by the secretion of lysozyme in addition to phagocytosis, a considerable fraction of the photocrosslinked chitosan appeared to remain in the bone defects even at 2 months. Similarly, the photocrosslinked chitosan hydrogel remained in lung (5) and gastric-submucosal layers (14) for several months with weak infiltration of neutrophils. The crosslinking of chitosan might cause its slower biodegradation.

In summary, we found that the photocrosslinkable chitosan hydrogel prevented bone formation. These findings suggested that the chitosan hydrogel might be a promising new suppressor for bone formation in the field of orthopedic surgery.

REFERENCES

1. Kamakura S, Nakajo S, Suzuki O, Sasano Y. New scaffold for recombinant human bone morphogenetic protein-2. *J Biomed Mater Res* 2004;71A:299–307.
2. Jupiter JB, Ring D. Operative treatment of post-traumatic proximal radioulnar synostosis. *J Bone Joint Surg* 1998; 80A:248–57.
3. Kanineni S, Maritz NG, Morrey BF. Proximal radial resection for posttraumatic radioulnar synostosis: a new technique to improve forearm rotation. *J Bone Joint Surg* 2002;84A:745–51.
4. Ono K, Saito Y, Yura H, et al. Photocrosslinkable chitosan as a biological adhesive. *J Biomed Mater Res* 2000;49:289–95.
5. Ono K, Ishihara M, Ozeki Y, et al. Experimental evaluation of photocrosslinkable chitosan as a biologic adhesive with surgical applications. *Surgery* 2001;130:844–50.

6. Einhorn TA. Clinically applied models of bone regeneration in tissue engineering research. *Clin Ortop* 1999;367s:s59–67.
7. Schmitz JP, Hollinger JO. The critical size defect as an experimental model for craniomandibulofacial nonunions. *Clin Ortop* 1986;205:299–308.
8. Ishihara M, Nakanishi K, Ono K, et al. Photocrosslinkable chitosan as a dressing for wound occlusion and accelerator in healing process. *Biomaterials* 2002;23:833–40.
9. Obara K, Ishihara M, Ishizuka T, et al. Photocrosslinkable chitosan hydrogel containing fibroblast growth factor-2 stimulates wound healing in healing-impaired db/db mice. *Biomaterials* 2003;24:3437–44.
10. Luo SM, Chang SJ, Chen TW, et al. Guided tissue regeneration for using a chitosan membrane: an experimental study in rats. *J Biomed Mater Res* 2006;76:408–15.
11. Shin SY, Park HN, Lee KH, et al. Biological evaluation of chitosan nanofiber membrane for guided bone regeneration. *J Periodontol* 2005;76:1778–84.
12. Seol YJ, Lee JY, Park JY, et al. Chitosan sponges as tissue engineering scaffolds for bone formation. *Biotechnol Lett* 2004;26:1037–41.
13. Tominaga K, Tominaga N, Tokuhisa M, et al. Influence of deacetylation of chitin on fibroblast-like cells and osteoblasts. *Jpn J Oral Maxillofac Surg* 1998;44:29–38.
14. Ishizuka T, Hayashi T, Ishihara M, et al. Submucosal injection, for endoscopic mucosal resection, of photocrosslinkable chitosan hydrogel in DMEM/F12 medium. *Endoscopy* 2007;39:428–33.

Rapid Communication

J. Biochem. 2009;145(3)275–278
doi:10.1093/jb/mvn169

Human Stem Cell Factor (SCF) is a Heparin-Binding Cytokine

Satoko Kishimoto[1,2], Shingo Nakamura[3], Hidemi Hattori[1], Shin-ichiro Nakamura[4], Fumie Oonuma[1], Yasuhiro Kanatani[1], Yoshihiro Tanaka[1], Yasutaka Mori[1], Yasuji Harada[2], Masahiro Tagawa[2] and Masayuki Ishihara[1,*]

[1]Research Institute, National Defense Medical College, 3-2 Namiki, Tokorozawa, Saitama 359-8513; [2]Department of Surgery, Graduate School of Nippon Veterinary Medicine and Life Science University, 1-7-1, Kyonan-cho, Musashino-shi, Tokyo, 180-8602; [3]Department of Surgery, National Defense Medical College, 3-2 Namiki, Tokorozawa; and [4]Department of Plastic and Reconstructive Surgery, National Defense Medical College, 3-2 Namiki, Tokorozawa, Saitama 359-8513, Japan

Received October 2, 2008; accepted December 2, 2008; published online December 12, 2008

Binding affinities of chemically modified heparins for human stem cell factor (SCF) were examined using fragmin/protamine microparticles (F/P MPs) and an enzyme-linked immunosorbent assay (ELISA). The binding of SCF to F/P MP-coated plates was inhibited with high concentrations of heparin and fragmin, but not others. The binding of SCF was also inhibited with 0.55 M or higher concentrations of NaCl in the medium. These results suggested that a high content of all three sulfate groups in repeating disaccharide units is required for interaction with SCF. Furthermore, pre-immobilized SCF on F/P MP-coated plates significantly stimulated proliferation of a human erythroleukemia cell line.

Key words: enzyme-linked immunosorbent assay (ELISA), fragmin/protamine microparticles (F/P MPs), heparin-binding cytokine, heparinoids, human stem cell factor (SCF).

Abbreviations: SCF, human stem cell factor; F/P MPs, fragmin (low-molecular-weight heparin)/protamine microparticles; ELISA, enzyme-linked immunosorbent assay; TF-1 cells, human erythroleukemia cell line; N-DS/N-Ac-H, N-desulfated, N-acetylated heparin; 2-O-DS-H, 2-O-desulfated heparin; 6-O-DS-H, 6-O-desulfated heparin.

Hematopoietic stem cells proliferate and mature in a niche consisting of semi-solid media when stimulated by exogenous hematopoietic cell growth factors (HCGFs) such as stem cell factor (SCF), interleukin (IL)-3, and granulocyte-macrophage colony-stimulating factor (GM-CSF), etc. In particular, SCF plays a key role in the regulation of hematopoiesis, acting as a regulator at various stages of this process. SCF promotes proliferation and early differentiation of cells at the level of multipotential stem cells. It has been suggested that SCF is essential for optimal production of various hematopoietic lineages, mainly because of its ability to prevent apoptosis when it co-stimulates with other cytokines (*1*). Hematopoietic stem cells also proliferate in association with bone marrow-derived stromal cells (*2*, *3*). In fact, it has been demonstrated that many natural and recombinant HCGFs such as IL-3, GM-CSF, etc. can be absorbed by heparinoids (heparin, heparan sulfate, modified heparin and other heparin-like molecules), which constitute the major sulfated glycosaminoglycans (GAGs) of bone marrow stroma (*2*, *3*). However, the heparin-binding character of SCF has not yet been elucidated.

We have prepared fragmin/protamine microparticles (F/P MPs) (about 1–0.5 μm in diameter) by mixing fragmin (low-molecular-weight heparin) as a heparinoid and protamine (*4*). Briefly, 0.3 ml of protamine solution (10 mg/ml; Mochida Pharmaceutical Co., Tokyo, Japan) was added drop by drop to 0.7 ml of fragmin solution (6.4 mg/ml; Kissei Pharmaceutical Co., Tokyo, Japan) with vortexing for 1 min. In order to maximize the production of microparticles, protamine and fragmin were mixed in a ratio of 3:7 (vol:vol) in this study. The F/P MPs, which constituted a milky solution, were then washed twice with phosphate-buffered saline (PBS) to remove non-reactants using centrifugation, and finally resuspended in 1 ml PBS. More than 7 mg of dry F/P MPs were obtained from 1 ml of F/P MPs milky solution. Although F/P MPs loosely bound to a plastic surface, the particles were easily rinsed away by washing. When the 24-well plate-bound F/P MPs were air-dried for 1 h on a clean bench, they were stably coated on the plastic surface.

IL-3 and GM-CSF are known to specifically bind to heparinoids (*5*), but it was previously unknown if SCF can bind to heparin. An enzyme-linked immunosorbent assay (ELISA) using cytokines (SCF, IL-3, and GM-CSF (R&D Systems Inc. Minneapolis, MN, USA)) and F/P MP-coated plates was performed to evaluate the adsorption of cytokines to the plates. Dulbecco's Modified Eagle's Medium (200 μl) (DMEM; Life Technologies Oriental, Tokyo, Japan) with indicated concentrations of those cytokines and 2% fetal bovine serum (FBS) was added to F/P MP-coated 48-well tissue culture plates (0.65 cm^2 of surface area) (Sumitomo Bakelite Corp., Tokyo, Japan), and the cytokines were bound to the plates at 37°C for 2 h. The plates were then washed

*To whom correspondence should be addressed: Tel: +81-42-995-1601, Fax: +81-42-991-1611, E-mail: ishihara@ndmc.ac.jp

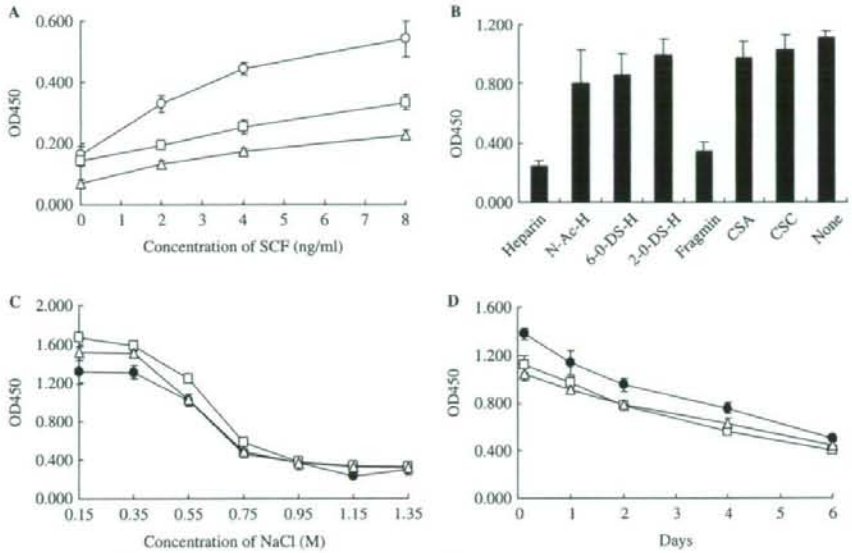

Fig. 1. **(A) Low FBS (2%) DMEM containing indicated concentrations of SCF was added to first F/P MP-coated plates (open circle) or non-coated plates (open triangle) and incubated at 37°C for 2 h.** The used medium was then added to second F/P MP-coated plates and incubated at 37°C for another 2 h (open square). (B) Various heparinoids and chondroitin sulfates (CSA and CSC) (200 μg/ml) were tested for their ability to competitively inhibit the binding of SCF to F/P MP-coated plates. C: Inhibitory effects of various concentrations of NaCl on the binding of SCF (filled circle), IL-3 (open square) and GM-CSF (open traingle) to F/P MP-coated plates. D: Release profile of SCF (filled circle), IL-3 (open square) and GM-CSF (open triangle) from pre-cytokine-immobilized F/P MP-coated plates. Amounts of immobilized cytokines were evaluated using an ELISA as described in text. Data represent mean ± SD of six determinations.

thoroughly with PBS/bovine serum albumin (0.1%) (BSA; Wako Pure Chemical Industries, Ltd., Osaka, Japan) three times. Diluted antibody (1:500 with PBS/BSA), anti-IL-3, anti-GM-CSF or anti-SCF (R&D Systems Inc.) was added to the plates, which were then incubated for 30 min at room temperature. Each well was again washed thoroughly with PBS/BSA and 200 μg/ml of anti-IgG horseradish peroxidase conjugate (diluted 1:1000 with PBS/BSA) (Bio-Rad Lab., Hercules, CA, USA) was added to the plates and incubated for 30 min at room temperature. Each well was again washed thoroughly with PBS/BSA, and the color was developed by adding 300 μl/ml of horseradish peroxidase substrate solution (Bio-Rad Lab.). The plates were mixed for 30 min and 50 μl of sulfuric acid (1 M) was finally added to each well to stop the reaction. The plates were read at 450 nm using a Mini Plate Reader (Nunc InterMed, Tokyo, Japan).

When 200 μl of various concentrations of SCF in DMEM with 2% FBS was added to F/P MP-coated 48-well tissue culture plates and incubated at 37°C for 2 h, SCF was detected on the plates in concentration-dependent manner by ELISA (Fig. 1A). Subsequently, the used culture medium was transferred into other F/P MP-coated plates and incubated once again at 37°C for 2 h. When the immobilized SCF in F/P MP-coated plates were measured by ELISA, the SCF levels of latter plates decreased to about 60% of the former plates. These results indicated that roughly 0.34 ng of SCF was immobilized onto the F/P MP-coated plates after incubating with 200 μl of 5 ng/ml SCF in DMEM with 2% FBS at 37°C for 2 h (Fig. 1A).

In order to measure the binding properties of SCF to heparinoid, various chemically modified heparins were evaluated for their ability to interact with SCF using ELISA and F/P MP-coated plates. Heparin and various chemically modified heparins which specifically bind to SCF should competitively inhibit the binding of SCF to the plates.

N-desulfated heparin was prepared according to the selective solvolytic method of Inoue and Nagasawa (*6*). The product was then converted to N-desulfated, N-acetylated heparin (N-DS/N-Ac-H) by N-acetylation procedures. Nitrous acid treatments at both pH 1.5 and pH 4 (*7*) did not cleave the product at all, indicating that N-desulfation and N-acetylation in those procedures were complete.

The 2-O-desulfated heparin (2-O-DS-H) (*8*) and 6-O-desulfated heparin (6-O-DS-H) (*9*) were prepared by methods reported previously. These procedures resulted in approximately 70% removal of 2-O-sulfates in 2-O-DS-H, 75% removal of 6-O-sulfates in 6-O-DS-H, and 95.4% removal of N-sulfates in N-DS/N-Ac-H (Table 1). Disaccharide compositional analyses of the chemically modified heparins were performed as described previously (*10*, *11*). Briefly, the polysaccharides (0.1 mg)

Table 1. **Disaccharide compositions of chemically modified heparins**

	Heparin (%)	Fragmin (%)	2-O-DS-H (%)	6-O-DS-H (%)	N-DS/N-Ac-H (%)
UA-GlcNAc	4.3	8.2	6.2	6.2	8.2
UA-GlcNS	3.8	7.2	20.5	5.3	0
UA-GlcAc(6-O-S)	0.7	0.5	2.9	0.3	8.7
UA(2-O-S)-GlcNAc	1.3	1.2	0	4.2	25.1
UA-GlcNS(6-O-S)	8.1	11.2	43.1	6.8	0.5
UA(2-O-S)-GlcNS	24.8	20.2	6.4	59.3	1.2
UA(2-O-S)- GlcNAc(6-O-S)	0	0	0	0.6	49.2
UA(2-O-S)- GlcNS(6-O-S)	52.6	47.2	14.4	12.7	2.9
Unknown	4.4	4.3	6.5	4.6	4.2

UA, uronate; GlcNAc, N-acetylglucosamine; GlcNS, N-sulfated glucosamine; UA(2-O-S), 2-O-sulfated uronate; GlcNAc(6-O-S), 6-O-sulfated N-acetylglucosamine; GlcNS(6-O-S), 6-O-sulfated N-sulfated glucosamine.

were treated with a mixture of heparinase (50 mU), heparitinase I (20 mU), and heparitinase II (20 mU) (Seikagaku Corp., Tokyo, Japan) in 220 µl of 2 mM calcium acetate and 20 mM sodium acetate (pH 7.0) at 37°C for 2 h. The completeness of the digestion was confirmed by gel-filtration chromatography with serially combined columns of TSK-Gel PW 4000, PW 3000 and PW 2500 (Tosoh Inc. Tokyo, Japan) using 0.2 M NaCl while monitoring absorbance at 230 nm and the refractive index for detection. The disaccharide composition was analyzed by ion-exchange chromatography of the reaction mixture with Dionex CarboPac PA-1 (4 × 250 nm). The gel-filtration chromatography showed no depolymerization for either 2-O-DS-H, 6-O-DS-H or N-DS/N-Ac-H.

As shown in Fig. 2B, heparin and fragmin at 200 µg/ml completely inhibited the binding of SCF to F/P MP-coated plates, while CSA, CSC, N-DS/N-Ac-H, 6-O-DS-H and 2-O-DS-H did not inhibit the binding even at concentrations of 400 µg/ml. We found that only a heparin-like molecule enriched in tri-sulfated disaccharide [UA(2-O-S)-GlcNS(6-O-S)] units (52.6% for heparin; 47.2% for fragmin) can competitively inhibit the binding of SCF to the F/P MP-coated plates; that is, only heparin-like molecules enriched in tri-sulfated disaccharide units (around 50%) can specifically interact with SCF. In contrast, chemically modified heparins enriched in di-sulfated disaccharide [UA-GlcNS(6-O-S), UA(2-O-S)-GlcNS and UA(2-O-S)-GlcNAc(6-O-S)] units have no inhibitory effect on binding. The inhibitory effects of heparin and fragmin for binding were concentration-dependent, and the half-inhibition concentrations were 25 and 35 µg/ml, respectively. These results suggest that SCF has affinity for heparin and fragmin, and that a high content of tri-sulfated (N-sulfate and 6-O-sulfate in GlcN residues and 2-O-sulfate in UA residues) disaccharide units is required for their interaction with SCF.

In the ELISA procedure, various concentrations of NaCl were tested for their ability to block the binding of the cytokines to F/P MP-coated plates. To inhibit the binding of SCF to the plates, 0.65 M NaCl was required. This requirement (0.65 M NaCl) is similar to that for GM-CSF (Fig. 1C). The binding of heparin-binding proteins to heparinoids can be blocked by high concentrations of NaCl, and the required concentration of NaCl is correlated with the affinity of the protein for heparinoid (*12*). To inhibit the binding of fibroblast growth factor (FGF)-1 and FGF-2 to F/P MP-coated plates, 1.05 M NaCl is required (*12*). On the other hand, the binding of hepatocyte growth factor (HGF) and IL-3 to the F/P MP-coated plates appears to be blocked with 0.75 M NaCl. Although the affinity of SCF for heparinoid is relatively low compared with other heparin-binding cytokines, the F/P MP-coated matrix efficiently adsorbed

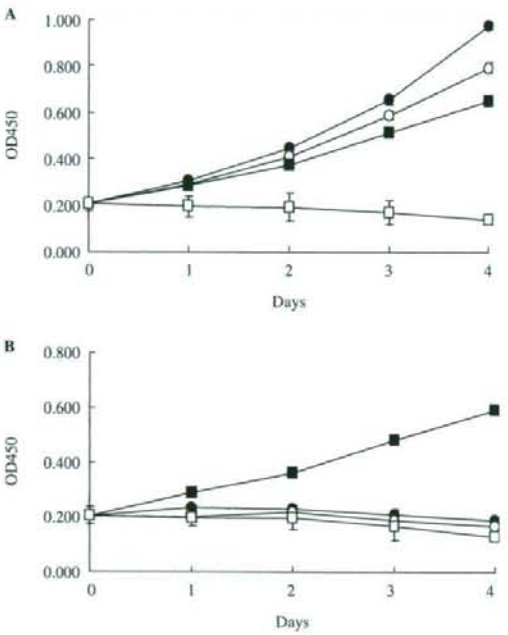

Fig. 2. **(A) TF-1 cells were cultured in low FBS (2%) DMEM with 5 ng/ml SCF either on F/P MP-coated plates (filled circle) or non-coated plates (open circle), and cultured in the same medium without SCF on pre-SCF-immobilized F/P MP-coated plate (filled square) or non-coated plates (open square).** (B) TF-1 cells were cultured in low FBS (2%) DMEM used to wash the pre-immobilized SCF for 2 days on F/P MP-coated plates (filled circle) or non-coated plates (open circle), and cultured in the same medium without SCF on the washed pre-SCF-immobilized F/P MP-coated plate (filled square) or non-coated plates (open square) for 2 days. Data represent mean ± SD of six determinations.

and stably retained SCF just as well as other heparin-binding cytokines.

It is recognized in polymer chemistry that positively and negatively charged polymers interact ionically. Basic protamine molecules complexed with acidic molecules (fragmin) form microparticles through ionic interactions (*4*). The F/P MPs are able to attach to polymeric surfaces such as plastic and glass, and they generate a stable paste-like coating upon complete drying as described in this study. It seems that SCF, once bound to F/P MP-coated plates, is gradually released from the coated surface *in vitro* with a half-life of 4–6 days (Fig. 1D). Furthermore, growth of TF-1 cells was stimulated both in low FBS (2%) DMEM (without SCF) on pre-SCF-immobilized F/P MP-coated plates and on non-coated plates using low FBS (2%) DMEM containing 5 ng/ml SCF (Fig. 2A). The medium to which the immobilized SCF was released for 2 days had little stimulatory effect on TF-1 cell growth (Fig. 2B). In contrast, TF-1 cell growth was significantly stimulated in low FBS (2%) DMEM (without SCF) on the pre-SCF-immobilized F/P MP-coated plates which were washed with low FBS (2%) DMEM (without SCF) for 2 days (Fig. 2B). Thus SCF immobilized onto F/P MP-coated plates appears to be bioactive for TF-1 growth. Our current study suggests that both the activity and stability of SCF are modified by the presence of heparin-like molecules which contain a high proportion of tri-sulfated disaccharide units. The molecular mechanism by which SCF is activated by interacting with F/P MP-coated plates is currently being investigated.

Heparinoids are known to bind various cytokines including FGFs, HGF, vascular endothelial growth factor, heparin-binding epidermal growth factor, platelet-derived growth factor, transforming growth factor-β, GM-CSF, interleukins (i.e. IL-1, IL-2, IL-3, IL-4, IL-6, IL-7 and IL-8), interferon γ and macrophage inflammatory protein-1, etc. (*13*, *14*). The present study suggests that SCF may be added to the list of heparin-binding cytokines.

CONFLICT OF INTEREST

None declared.

REFERENCES

1. Pesce, M., Farrace, M.G., Piacentini, M., Dolci, S. and Felici, M. (1993) Stem cell factor and leukemia inhibitory factor promote primordial germ cell survival by suppressing programmed cell death (apoptosis). *Development* **118**, 1089–1094
2. Roberts, R., Gallagher, J., Spooncer, E., Allen, T.D., Bloomfield, F., and Dexter, T.M. (1988) Heparan sulfate bound growth factors: a mechanism for stromal cell mediated haemopoiesis. *Nature* **332**, 376–378
3. Gordon, M.Y., Riley, G.P., Watt, S.M., and Greaves, M.F. (1987) Compartmentalization of a haematopoietic growth factor (GM-CSF) by glycosaminoglycans in the bone marrow microenvironment. *Nature* **326**, 403–405
4. Nakamura, S., Kanatani, Y., Kishimoto, S., Nambu, M., Ohno, C., Hattori, H., Takase, B., Tanaka, Y., Kiyosawa, T., Maehara, T., and Ishihara, M. (2008) Controlled release of FGF-2 using fragmin/protamine microparticles and effect on neovascularization. *J. Biomed. Mater. Res. A.* (in press)
5. Alvarez-Silva, M. and Borojevic, R. (1996) GM-CSF and IL-3 activities in schistosomal liver granulomas are controlled by stroma-associated heparan sulfate proteoglycans. *J. Leukoc. Biol.* **59**, 435–441
6. Inoue, Y. and Nagasawa, K. (1976) Selective N-desulfation of heparin with demethyl sulfoxide containing water and methanol. *Carbohydr. Res.* **46**, 87–95
7. Guo, Y.C. and Conrad, H.E. (1989) The disaccharide composition of heparins and heparan sulfate. *Anal. Biochem.* **176**, 96–104
8. Piani, S., Casu, B., Marchi, E.G., Torri, G., and Ungarelli, F. (1993) Alkali-induced optical rotation changes in heparins and heparan sulfates, and their relation to iduronic acid-containing sequences. *J. Carbohydr. Chem.* **12**, 507–521
9. Takano, R., Kanda, T., Hayashi, K., Yoshida, K., and Hara, S. (1995) Desulfation of sulfated carbohydrates mediated by silyating reagents. *J. Carbohydr. Chem.* **14**, 885–888
10. Yoshida, K., Miyauchi, S., Kikuchi, H., Tawada, A., and Tokuyasu, K. (1989) Analysis of unsaturated disaccharides from glucosaminoglycuronan by high-performance liquid chromatography. *Anal. Biochem.* **177**, 327–332
11. Kariya, Y., Yoshida, K., Morikawa, K., Tawada, A., Miyazono, H., Kikuchi, H., and Tokuyasu, K. (1992) Preparation of unsaturated disaccharides by eliminative cleavage of heparin and heparin sulfate with heparitinases. *Comp. Biochem. Physiol. B.* **103**, 473–479
12. Ishihara, M., Tyrrell, D.J., Stauber, G.B., Brown, S., Cousens, L.S., and Stack, R.J. (1993) Preparation of affinity-fractionated, heparin-derived oligosaccharide and their effects on selected biological activities mediated by basic fibroblast growth factor. *J. Biol. Chem.* **268**, 4675–4683
13. Salmivirta, M., Lidholt, K., and Lindahl, U. (1996) Heparan sulfate: a piece of information. *FASEB J.* **10**, 1270–1279
14. Lindahl, U., Lidholt, K., Spillmann, D., and Kjellen, L. (1994) More to "heparin" than anticoagulation. *Thromb. Res.* **75**, 1–32

Experimental evaluation of photocrosslinkable chitosan hydrogel as injection solution for endoscopic resection

Authors T. Ishizuka[1], M. Ishihara[2], S. Aiko[1], Y. Nogami[1], S. Nakamura[1], Y. Kanatani[2], S. Kishimoto[2], H. Hattori[2], T. Horio[1], Y. Tanaka[2], T. Maehara[1]

Institutions [1] Dept. of Surgery, National Defense Medical College, Tokorozawa, Saitama, Japan
[2] Research Institute, National Defense Medical College, Tokorozawa, Saitama, Japan

submitted 22 January 2008
accepted after revision 13 October 2008

Bibliography
DOI 10.1055/s-0028-1103483
Endoscopy 2009; 41: 25–28 © Georg Thieme Verlag KG Stuttgart · New York
ISSN 0013-726X

Corresponding author
M. Maehara, MD
Department of Surgery
National Defense Medical College
3-2 Namiki
Tokorozawa, Saitama
359-8513 Japan
Fax: +81-429-91-1611
maeharat57@yahoo.co.jp

Background and study aims: Saline as an injection solution for endoscopic resection techniques has several disadvantages such as a short-lasting effect leading to a potentially higher risk of bleeding and perforation. The new substance of photocrosslinkable chitosan hydrogel in a DMEM/F12 medium (PCH) can be converted into an insoluble hydrogel by ultraviolet irradiation for 30 s, and was evaluated in two sets of animal experiments.
Methods: 18 pigs were used in the two parts of the study. First, mucosal resections were done with either PCH or hypertonic saline; the effects of both agents on wound healing were examined endoscopically and histologically. Second, in vivo degradation of PCH was examined using six pig stomachs.
Result: PCH injection led to a longer-lasting elevation with clearer margins, compared with hypertonic saline, thus enabling precise endoscopic submucosal dissection (ESD) along the margins of the elevated mucosa. The endoscopic appearance after ESD was similar in both groups. PCH biodegradation was completed within 8 weeks according to endoscopic and histologic analyses.
Conclusion: PCH is a promising agent for submucosal injection prior to various techniques of endoresection. It should be evaluated in clinical trials after biocompatibility testing for PCH is completed.

Introduction

Saline-assisted endoscopic mucosal resection (EMR) is an established therapy with low invasion. En bloc resection of the lesion and histopathological analysis are required to evaluate curativeness [1]. However, complete resection of lesions larger than 2 cm in diameter is still difficult [2], even though EMR techniques have been improved [3,4]. The development of endoscopic submucosal dissection (ESD) has raised the success rate for en bloc resection, but perforation occurs more frequently in the course of ESD than during EMR [5].

Photocrosslinkable chitosan in DMEM/F12 medium (PCH) is a viscous solution that crosslinks upon ultraviolet irradiation, resulting in an insoluble hydrogel. The substantial effects of PCH have been observed in significant granulation tissue formation and vascularization in vivo, as has the significant neutrophil infiltration and biodegradation of PCH [6,7]. In a previous study of rats, we reported that PCH was a useful submucosal injection agent [8]. The aims of the present study, using pigs, were to investigate the feasibility and safety of PCH-assisted ESD and to evaluate the in vivo biodegradation of PCH.

Materials and methods

Photocrosslinkable chitosan hydrogel in DMEM/F12 medium (PCH)

Photocrosslinkable chitosan hydrogel was prepared as described previously [9]. In brief, the chitosan (Yaizu Suisankagaku Industry Co., Shizuoka, Japan) had a molecular weight of 800 – 1000 kDa, and was 80% deacetylated. Azide (p-azido-benzoic acid) and lactose (lactobionic acid) moieties had been introduced to the amino group and about 2.5% and 2% of the amino groups in the chitosan had been replaced by p-azidobenzoic acid and lactobionic acid, respectively.

In this study, 0.75% PCH was prepared by dissolving the lyophilized photocrosslinkable chitosan hydrogel with DMEM/F12 medium (GIBCO Life Sciences Corp., Grand Island, New York, USA). This solution (PCH) was converted into an insoluble hydrogel by 30 s of ultraviolet irradiation at a lamp distance of 2 cm (250 W lamp, MUV-250U-

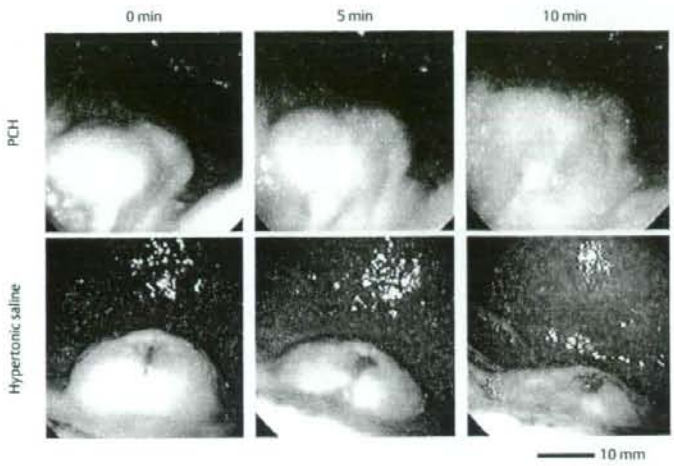

Fig. 1 Endoscopic appearance after the injection of photocrosslinkable hydrogel PCH (upper panel) and hypertonic saline (bottom panel) in living porcine stomachs, immediately after injection (left), after 5 min (center), and after 10 min (right).

L; Moritex Co., Saitama, Japan), through crosslinking of the azide and amino groups of PCH.

PCH-assisted endoscopic submucosal dissection (ESD)

Animal experiments were carried out according to the protocol approved by the Animal Experimentation Committee of the National Defense Medical College (Saitama, Japan). The two experimental groups consisted of six pigs each (stockbreeding pigs, 50–60 days, all male, average weight 20 kg; Saitama Experimental Animals Supply Co. Ltd, Saitama, Japan). After 2 days of fasting, pigs were sedated with ketamine (50 mg/kg intramuscularly) and then anesthetized with a bolus of sodium pentobarbitone (induction 20 mg/kg intravenously), followed by continuous infusion (5 mg/kg/h intravenously). Endoscopic procedures were performed with the animals under anesthesia receiving general mechanical ventilation.

We used a single-accessory channel endoscope for animals (Olympus VQ-8143A; Tokyo, Japan). Using a 23-gauge injection needle (Olympus NM-200U-0423) passed through the endoscopic accessory channel, mucosal elevations were created by submucosal injection of 5 ml of either 10% hypertonic saline (Ohtsuka Pharm., Tokushima, Japan) or 0.75% PCH. When PCH was injected, ultraviolet irradiation was applied over the elevated mucosa for 1 min, using an ultraviolet lamp system (MUV-250U-L; Moritex Co. Japan) and the ultraviolet light-fiber for EMR (AFP01437; Moritex Co. Japan) passed through the endoscopic accessory channel. The submucosal injection of 0.75% PCH was done using an endoscopic injection needle and a small-caliber syringe (3 ml).

One group of pigs underwent PCH-assisted ESD while the other underwent hypertonic saline-assisted ESD. Markings for the incision line were placed 5–10 mm outside the margin of the 3 cm diameter mucosal resection area, with a needle-knife (Olympus KD-620 LR) and an electrosurgical current generator (Olympus PSD-60) set at 15 W for forced coagulation mode. PCH was then injected through an endoscopic injection needle to the submucosal layer of the distal margin, and ultraviolet irradiation was applied over the elevated mucosa, as described above. A mucosal incision was then made with a needle-knife around the distal margin of the mucosal resection area. Submucosal injection and ultraviolet irradiation of the proximal margin of mucosal resection area were done in the same way as at the distal margin. Finally, a circumferential mucosal incision was made with the needle-knife.

As a control, hypertonic saline-assisted ESDs (n = 6) were carried out using the same single-accessory channel endoscope (Olympus VQ-8143A), another attachable channel (Olympus VH-114-CH), a needle-knife (Olympus KD-620 LR) for precut, and an insulated-tip (IT) knife (Olympus KD-610 L).

The artificial ulcers produced by either hypertonic saline-assisted or PCH-assisted ESD were observed, and the lengths of the artificial ulcers were endoscopically measured at 1 and 4 weeks after the ESD procedures.

Histological examination

The animals were sacrificed by means of an anesthesia overdose at 8 weeks and their stomachs were resected for the preparation of histological specimens. The tissues were then fixed in 10% formalin for 2 days, embedded in paraffin and sectioned, followed by staining with hematoxylin and eosin (H&E) reagents.

Biodegradation of PCH injected into the submucosa

In vivo degradation of PCH was examined using six pig stomachs. After an injection of 5 ml of 0.75% PCH endoscopically and ultraviolet irradiation over the elevated mucosa, which was not followed by resection of the mucosa, the biodegradation was endoscopically observed at 1, 4, and 8 weeks after the application of PCH. Finally three animals were sacrificed by means of an anesthesia overdose at 4 weeks and three at 8 weeks, and their stomachs were resected for the preparation of histological specimens.

Results

Elevation of the submucosal layer

The changes in elevations at the injection sites were observed endoscopically at 0, 5, 10, 30, and 60 min after the injections (**Fig. 1**).

The margin of the elevated mucosa became indistinct within 5 min after the injection of hypertonic saline, and the elevation collapsed after 10 min. Where PCH had been injected, the shape

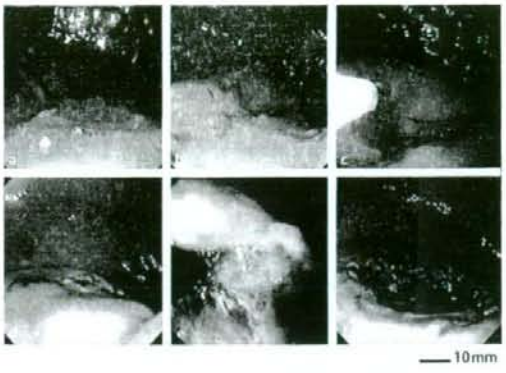

Fig. 2 Endoscopic images of PCH-assisted endoscopic submucosal dissection (ESD). **a** Marking. **b** Elevation of the distal margin of the mucosal resection area by submucosal injection of PCH. **c** Irradiation with ultraviolet. **d** Elevation of the proximal margin of the mucosal resection area. **e** Incision using the needle knife. **f** Artificial ulcer after mucosal resection.

Fig. 3 Changes in endoscopic appearance after mucosal resection using PCH-assisted ESD (upper panel) and hypertonic saline-assisted ESD (bottom panel) in living porcine stomach, immediately after resection (left), after 1 week (center), and after 4 weeks (right).

of the elevated mucosa was unchanged for more than 3 h (data not shown). We attribute this difference to the properties of the PCH which had the viscosity of soft rubber following ultraviolet irradiation for 1 min [6,7].

PCH-assisted ESD

The PCH-assisted ESD procedures (n = 6) were carried out by endoscopic injection of 5 ml of 0.75 % PCH and two incisions of the elevated mucosa (the distal and the proximal margins of the mucosa) (**Fig. 2**).

Most of the injected and irradiated PCH could be removed with the resected mucosa. Thus, there was little residual PCH in the artificial ulcers (about 3 cm in diameter) as observed endoscopically. No complications were observed in the PCH-assisted ESD procedures.

In contrast, the elevation rapidly collapsed in hypertonic saline-assisted ESD procedures. Thus, it was difficult to resect the 3-cm diameter elevated mucosa because submucosal dissection had to be used in hypertonic saline-assisted procedures.

The areas of the resected mucosa were $16.2 \pm 1.78\ mm^2$ and $15.8 \pm 1.25\ mm^2$ with PCH-assisted ESD and hypertonic saline-assisted ESD, respectively. The volume of submucosal injection fluid was 10.1 ± 1.60 ml for PCH-assisted ESD and 12.0 ± 1.79 ml with hypertonic saline-assisted ESD. In addition, minor bleedings were observed several times in the course of hypertonic saline-assisted ESD procedures (data not shown).

Wound healing after PCH-assisted ESD

After 1 week the artificial ulcers generated from both PCH-assisted and hypertonic saline-assisted ESD exhibited an early healing stage with some edematous changes in the surrounding mucosa. The extent of wound closure was 23.4 ± 5.8 % in PCH-assisted ESD lesions, and was 19.0 ± 10.3 % in hypertonic saline-assisted ESD lesions; these results were not significantly different. After 4 weeks, the surfaces of the artificial ulcers created by PCH-assisted ESD were covered with regenerated mucosa but mucosal folds remained (**Fig. 3**), similar to those seen with hypertonic saline-assisted ESD.

Biodegradation of PCH injected into the submucosa

In vivo degradation of PCH was examined endoscopically and pathologically. The sites at which PCH had been applied were reduced in size after 4 weeks and only mucosal folds were endoscopically observed at 8 weeks (**Fig. 4a**). In the pathological examinations, a small amount of PCH could be observed after 4 weeks, but it had completely disappeared after 8 weeks (**Fig. 4b**).

Discussion

EMR has been widely accepted as a standard local treatment for superficial neoplastic lesions in the alimentary tract [10,11] since the development of the strip biopsy method in 1984 [12]. The use of a submucosal injection agent, such as hypertonic saline with epinephrine [1], 50% glucose [13], sodium hyarulonate [14–16], or hydroxypropyl methylcellulose [17] can help to prevent major complications from the EMR procedure. A sufficient volume of the injection solution must be maintained in the submucosa until the lesion is removed. En bloc resection of a large lesion is often not achieved by conventional EMR, but the development of ESD allowed en bloc resection of extensive lesions [5,18]. However, ESD requires a high level of technical skill and the frequency of complications caused by ESD is higher than that for conventional EMR [5,18].

We have previously reported that PCH is a useful submucosal injection agent [8]. Because this viscous solution is converted into an insoluble, flexible hydrogel with the consistency of soft rubber, it can maintain good mucosal elevation and physically prevent bleeding from the artificial ulcers.

In the case of PCH-assisted ESD, submucosal injections and incisions were done at two different sites of the area to be resected (**Fig. 2**), because incision at the distal margin of the elevated mucosa had to be performed blindly. PCH-assisted ESDs have many advantages compared with conventional EMR and ESD. Techniques for PCH-assisted ESD are simple and relatively easy since this method needs only two injection sites, ultraviolet irradiation, and incision without submucosal dissection. En bloc resection can be done, and accurate pathological diagnosis can be made. During the mucosal incision, there was no minor bleeding

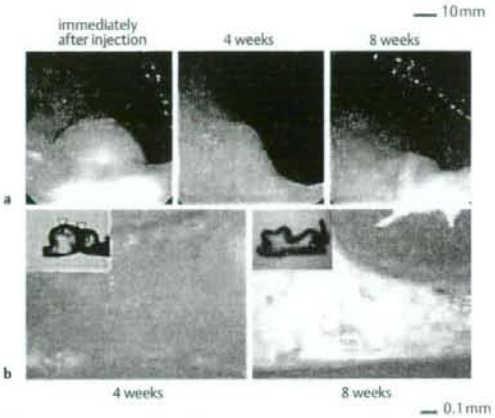

Fig. 4 In vivo degradation of PCH. **a** Endoscopic appearance of elevated mucosal areas following injection of 5 ml of PCH, immediately after application, 4 weeks later, and 8 weeks later. PCH application sites revealed only mucosal folds after 8 weeks. **b** Histological appearance of PCH application sites at 4 and 8 weeks. Although minor residual PCH was observed at 4 weeks, none was observed at 8 weeks. The triangles represent residual PCH.

at the site of the artificial ulcers. Perforation was prevented by the application of PCH. This is because insoluble PCH seems to prevent the electrosurgical current from entering the muscle layer. PCH-assisted ESD can be done using a single-accessory channel endoscope without using special devices or a polypectomy snare. Regarding application in the human stomach, PCH-assisted ESD could be used for early cancer of the cardia, as bleeding is prevented. On the other hand, hypertonic saline-assisted ESD might not be applied to large lesions (over 3 cm in diameter). In addition, the feasibility of PCH-assisted ESD in pig esophagus and colon is now under investigation.

With regard to wound healing, conventional chitosan reduces ethanol-induced gastric mucosal injury and accelerates the healing of acetic acid-induced gastric ulcers in rats [19]. Chitosan hydrogel also induces wound contraction and accelerates wound closure and healing in skin [20, 21]. These characteristics of PCH are useful for healing of artificial ulcers after EMR and ESD [8, 22]. However, a significant stimulation of wound healing after PCH-assisted ESD was not observed in this study. These results were probably due to the strong adhesion of injected PCH to the dissected mucosal tissue; thereby, none of the PCH remained within the wounds.

PCH is nontoxic for human skin fibroblasts, human endothelial cells, and human smooth muscle cells [9]. In vivo degradation of PCH has been observed at the injection site in rat stomach [8]. In the present study, applied PCH also appeared to be biodegraded within 8 weeks (**O Fig. 4**). These results suggest that PCH is safe for use as a submucosal injection agent, although more detailed toxicity testing in appropriate animal models remains to be performed. The ultraviolet radiation may be associated with the inflammation of residual tissue. However, it can be predicted that ultraviolet irradiation for PCH-assisted ESD might not have any association with carcinogenesis though further study will be required.

In conclusion, PCH-assisted ESD can be performed using a single-accessory channel endoscope and without any special devices. This submucosal injection agent may permit reliable ESD without complications such as bleeding and perforation. It should be evaluated in clinical trials after biocompatibility testing for PCH has been completed.

Competing interests: None

References

1 *Hirano M, Masuda K, Asanuma T et al.* Endoscopic resection of early gastric cancer and other tumors with local injection of hypertonic saline-epinephrine. Gastrointest Endosc 1988; 34: 264 – 269
2 *Tada M, Inoue H, Yabata E et al.* Colonoscopic mucosal resection using a transparent cap-fitted endoscope. Gastroentest Endosc 1996; 44: 63 – 65
3 *Inoue H, Kawano T, Tani M et al.* Endoscopic mucosal resection using a cap: techniques for use and preventing perforation. Can J Gastroentrol 1999; 13: 477 – 480
4 *Suzuki H.* Endoscopic mucosal resection using ligating device for early gastric cancer. Gastrointest Endosc Clin N Am 2001; 11: 511 – 518
5 *Fujishiro M, Yahagi N, Kashimura K et al.* Tissue damage of different submucosal injection solutions for EMR. Gastrointest Endosc 2005; 62: 933 – 942
6 *Kiyozumi T, Kanatani Y, Ishihara M et al.* The effect of chitosan hydrogel containing DMEM/F12 medium on full-thickness skin defects after deep dermal burn. Burns 2007; 33: 642 – 648
7 *Kiyozumi T, Kanatani Y, Ishihara M et al.* Medium (DMEM/F12)-containing chitosan hydrogel as adhesive and dressing in autologous skin grafts and accelerator in the healing process. J Biomed Mater Res 2006; 79B : 129 – 136
8 *Ishizuka T, Hayashi T, Ishihara M et al.* Submucosal injection, for endoscopic mucosal resection, of photocrosslinkable chitosan hydrogel in DMEM/F12 medium. Endoscopy 2007; 39: 428 – 433
9 *Ono K, Saito Y, Yura H et al.* Photo-crosslinkable chitosan as a biological adhesive. J Biomed Res 2000; 49: 289 – 295
10 *Inoue H.* Endoscopic mucosal resection for the entire gastrointestinal mucosal lesions. Gsatrointest Endosc Clin N Am 2001; 11: 459 – 478
11 *Takekoshi T, Baba Y, Ota H et al.* Endoscopic resection of early gastric carcinoma; results of a retrospective analysis of 308 cases. Endoscopy 1994; 26: 352 – 358
12 *Tada M, Shimada M, Murakami F et al.* Development of the strip-off biopsy. Gastroenterol Endosc 1984; 26: 833 – 839
13 *Makuuchi H, Mitomi T, Machimura T et al.* Endoscopic mucosal resection for early esophageal cancer by EMR-tube method. Stomach Intest 1988; 28: 153 – 159
14 *Yamamoto H, Yube T, Isoda N et al.* A novel method of endoscopic mucosal resection using sodium hyaluronate. Gastrointest Endosc 1999; 50: 251 – 256
15 *Yamamoto H, Koiwai H, Yube T et al.* A successful single-step endoscopic resection of a 40 millimeter flat-elevated tumor in the rectum: endoscopic mucosal resection using sodium hyaluronate. Gastrointest Endosc 1999; 50: 701 – 704
16 *Yamamoto H, Kawata H, Sunada K et al.* Successful en bloc resection of large superficial tumors in the stomach and colon using sodium hyaluronate and small-caliber-tip transparent hood. Endoscopy 2003; 35: 690 – 694
17 *Feitoza AB, Gostout CJ, Burgard LJ et al.* Hydroxypropyl methylcellulose: a better subumcosal fluid cushion for mucosal resection. Gastrointest Endosc 2003; 57: 41 – 47
18 *Fujishiro M.* Endoscopic submucosal dissection for stomach neoplasms. W J Gastroendosc 2006; 12: 5108 – 5112
19 *Ito M, Ban A, Ishihara M et al.* Anti-ulcer effects of chitin and chitosan, healthy foods, in rats. Jpn J Pharmacol 2000; 82: 218 – 225
20 *Ishihara M, Nakanishi K, Ono K et al.* Photo-crosslinkable chitosan as a dressing for wound occlusion and accelerator in healing process. Biomaterials 2002; 23: 833 – 840
21 *Ishihara M, Ono K, Sato M et al.* Acceleration of wound contraction and healing with a photocrosslinkable chitosan hydrogel. Wound Rep Regen 2001; 9: 513 – 521
22 *Hayashi T, Matsuyama T, Hanada K et al.* Usefulness of photoclosslinkable chitosan for endoscopic cancer treatment in alimentary tract. J Biomed Mater Res B Appl Biomater 2004; 71: 367 – 372

4. Tatsumi E, Takano H, Taenaka Y, et al. Development of an ultracompact integrated heart–lung assist device. *Artif Organs* 1999;23:518–23.
5. Taga I, Funakubo A, Fukui Y. Design and development of an artificial implantable lung using multiobjective genetic algorithm: evaluation of gas exchange performance. *ASAIO J* 2005;51:92–102.
6. Funakubo A, Taga I, McGillicuddy JW, Fukui Y, Hirschl RB, Bartlett RH. Flow vectorial analysis in an artificial implantable lung. *ASAIO J* 2003;49:383–7.
7. Ishimaru A. *Wave Propagation and Scattering in Random Media*. New York: IEEE Press, 1997.
8. Jonson CC. Optical diffusion in blood. *IEEE Trans Biomed Eng* 1970;17:129–34.
9. Reynolds LO, Johnson CC, Ishimaru A. Diffuse reflectance from a finite blood medium, applications to the modeling of fiber optic catheters. *Appl Opt* 1976;15:2058–67.
10. Takatani S, Graham MD. Theoretical analysis of diffuse reflectance from a two layer tissue model. *IEEE Trans Biomed Eng* 1979;26:656–64.
11. Steinke JM, Shepherd AP. Role of light scattering in whole blood oximetry. *IEEE Trans Biomed Eng* 1986;33:294–301.
12. Schmitt JM, Meindl JD, Mihm FG. An integrated circuit-based optical sensor for in vivo measurement of blood oxygenation. *IEEE Trans Biomed Eng* 1986;33:98–107.
13. Polanyi RM, Hehir RM. In vivo oximeter with fast dynamic response. *Rev Sci Instrum* 1962;33:1050–4.
14. Chance B, Wang NG, Maris M, Nioka S, Sevick E. Quantitation of Tissue Optical Characteristics and Hemoglobin Desaturation by Time—and Frequency—Resolved Multiwave Length Spectrophotometry. *Adv Exp Med Biol* 1992;297–304.
15. Mannheimer PD, Casciani JR, Fein ME. Wavelength selection for lower saturation pulse oximetry. *IEEE Trans Biomed Eng* 1997;44:148–58.

A Tissue-engineered Stomach Shows Presence of Proton Pump and G-cells in a Rat Model, Resulting in Improved Anemia Following Total Gastrectomy

*†Tomoyuki Maemura, ‡Michael Shin, *Manabu Kinoshita, †Takashi Majima, §Masayuki Ishihara, *Daizoh Saitoh, and †Takashi Ichikura

*Division of Traumatology, National Defense Medical College Research Institute, Saitama; †Department of Surgery, National Defense Medical College, Saitama, Japan; ‡Department of Surgery, Massachusetts General Hospital and Harvard Medical School, Boston, MA, USA; and §Division of Biomedical Engineering, National Defense Medical College Research Institute, Saitama, Japan

doi:10.1111/j.1525-1594.2007.00528.x

Received December 2006; revised July 2007.

Address correspondence and reprint requests to Dr. Tomoyuki Maemura, Division of Traumatology, National Defense Medical College Research Institute, Namiki 3-2, Tokorozawa 359-8513, Japan. E-mail: manabu@ndmc.ac.jp

Abstract: Despite advances in surgical reconstruction, total gastrectomy still is accompanied by various complications, especially chronic ones, such as pernicious anemia, resulting in refractory malnutrition. As an alternative approach, we have proposed a tissue-engineered stomach as a replacement of the native stomach. This study aimed to assess the secretory functions of a tissue-engineered stomach in a rat model and the nutritional status of the recipients over an extended time period. Stomach epithelial organoid units were isolated from neonatal rats and seeded onto biodegradable polymers. These constructs were implanted into the omenta of adult recipient rats. After 3 weeks, cyst-like structures had formed, henceforth referred to as tissue-engineered stomachs. The recipient stomachs were resected and replaced by their tissue-engineered counterparts. At 24 weeks after implantation, the secretory function of the tissue-engineered stomach was evaluated using immunohistochemical staining. The hemoglobin levels and nutritional status of the recipients were compared with a control group that had undergone a simple Roux-en-Y reconstruction following total gastrectomy. Recipient rats tolerated the tissue-engineered stomachs well. X-ray examination using barium as contrast showed no bowel stenosis. Staining for proton pump α-subunit and gastrin demonstrated the existence of parietal cells and G-cells in the neogastric mucosa, respectively, suggesting secretory functions. The treatment group showed significantly higher hemoglobin levels than the control group, although no differences in the body weight change, total protein, or cholesterol levels were observed between the two groups. A tissue-engineered stomach has the potential to function as a food reservoir following total gastrectomy. It is conjectured that replacement with a tissue-engineered stomach might restore the proton pump parietal cells and G-cells, and thereby improve anemia after a total gastrectomy in a rat model. **Key Words:** Tissue-engineered stomach—Total gastrectomy—Pernicious anemia.

The best reconstruction mode following a total gastrectomy has not been identified yet, because no substitutes possess gastric mucosal cells such as the parietal or G-cells. Pernicious anemia usually occurs in patients after a total gastrectomy due to the abrogation of parietal cells that exclusively produce the intrinsic factor, which is essential to absorb vitamin B-12. The patients therefore deplete the storage of vitamin B-12 within a few years after a total gastrectomy and require vitamin B-12 supplements via intravenous or intramuscular injection on a semipermanent basis.

It is argued that restoration of the parietal and G-cells is indispensable to prevent pernicious anemia following a total gastrectomy. Our laboratory has investigated the use of a tissue-engineered stomach as an alternative approach to a total gastrectomy (1–3). Here, we present a study on the effectiveness of a tissue-engineered stomach over an extended time frame (24 weeks) after a total gastrectomy focusing on restoration of the parietal cells and

G-cells and prevention of refractory malnutrition including pernicious anemia.

MATERIALS AND METHODS

Fabrication of tissue-engineered stomachs

Tissue-engineered stomachs were prepared as previously described (1,2). Briefly, organoid units of stomach epithelium were isolated from neonatal Lewis rats (Charles River Laboratories, Wilmington, MA, USA). Following euthanasia with methoxyflurane, whole stomachs were harvested, stripped of the omentum, and placed in cold Hank's balanced salt solution (HBSS) (Cellgro, Herndon, VA, USA). The stomachs were opened, and the contents were removed. The forestomachs, consisting of stratified squamous epithelium, were removed to isolate the area consisting of columnar epithelium. Each stomach was washed seven times with HBSS to remove debris and mucus. Thereafter, the lavaged stomachs were minced into less than 1 mm^3 pieces with sterile scalpel blades. The tissue fragments were enzymatically digested with dispase I (0.1 mg/mL, neural protease type I, Boehringer Ingelheim GmbH, Ingelheim, Germany) and collagenase XI (300 U/mL, *Clostridium histolycium* type XI, Sigma-Aldrich, St. Louis, MO, USA) at room temperature on an orbital shaker at 80 cycles/min for 25 min. The stomach epithelium organoid units were further purified by centrifugation in a solution of Dulbecco's modified Eagle medium (Gibco, Gaithersburg, MD, USA) supplemented with 2.5% fetal calf serum (Sigma-Aldrich), and 2% sorbitol (Sigma-Aldrich) at 300 rpm for 2 min.

Microporous biodegradable polymer tubes (10 mm length, 5 mm outer diameter, 2 mm inner diameter) were made from a fibrous, nonwoven polyglycolic acid (PGA) mesh (15 μm fiber diameter, porosity >95%; Smith & Nephew, Heslington, York, UK), coated with 5% poly(L-lactic acid) (Sigma) in chloroform. Prior to seeding, the polymer tubes were coated with type I collagen (Vitrogen 100, Cohesion Technologies, Palo Alto, CA, USA) to improve cell attachment. The isolated stomach epithelium organoid units were resuspended and seeded onto the inner luminal surface of each polymer tube at a density of $1–3 \times 10^4$ units/tube. The stomach epithelium organoid units were allowed to attach to the polymer for 1 h prior to implantation. Syngeneic adult rats (200–250 g) were used as recipients. Under ketamine/xylazine anesthesia, the recipients underwent an upper midline incision and the omenta were exposed. The seeded polymer tubes were wrapped completely into the omentum, secured with suture, and placed back into the abdominal cavity. The abdominal cavities were closed in two layers with suture. The animals were maintained in a temperature-regulated environment on a 12-h light–dark cycle, and given access to rat chow and tap water ad libitum. The status and well-being of the animals were checked daily.

Replacement surgery

Three weeks after implantation, cystic structures had formed. The recipients ($n = 15$) underwent a second operation for the replacement of the native stomach. A midline incision was performed, and the cyst, henceforth referred to as tissue-engineered stomach, was exposed. The caudal side of the tissue-engineered stomach was opened longitudinally, and the contents were removed. The caudal side of the tissue-engineered stomach was anastomosed to the native jejunum at the 5 cm distal site to the ligament of Treitz in a side-to-side fashion. The omentum was preserved to maintain blood supply to the tissue-engineered stomach, and the native stomach was resected. The proximal side of the duodenum was closed to be a stump. A hole for anastomosis was made at the cephalic side of the tissue-engineered stomach. The cephalic side of the tissue-engineered stomach was anastomosed to the native esophagus in the abdominal cavity in an end-to-end fashion. The abdominal cavity was closed in two layers with suture.

The control group consisted of rats that underwent a simple Roux-en-Y reconstruction in conjunction with a total gastrectomy ($n = 3$). The jejunum was dissected at 4 cm distal from the ligament of Treitz, and its distal end was brought up in an antecolic position for an esophagojejunostomy in an end-to-end fashion. Bile and pancreatic juice were diverted at 10 cm below the esophagojejunostomy in an end-to-side fashion. The proximal side of the duodenum was closed to be a stump.

Assessment

The body weights of recipients were measured every day for 24 weeks following the replacement surgery. At 24 weeks, all recipients underwent an upper gastrointestinal study. Under anesthesia, a silicone tube was cannulated into the esophagus, and 10 mL of barium solution was injected. The animals were observed, and X-rays were taken for 30 min at 5-min intervals. Subsequently, the rats were sacrificed, and the tissue-engineered stomachs with native esophagus and jejunum were harvested for histological examination. The volumes of the tissue-engineered stomachs were measured by applying ligations just